# MC Simulation of Aerosol Aggregation and Simultaneous Spheroidization

**Daniel E. Rosner and Suyuan Yu**
Chemical Engineering Dept., High Temperature Chemical Reaction Engineering Laboratory, Yale University, New Haven, CT 06520

*A companion article by Tandon and Rosner (1999) showed that Monte-Carlo (MC) simulation methods can generate joint pdfs of particle volume, $v$, and surface area, $a$, for coagulating populations of suspended nonspherical particles simultaneously sintering at finite rates. For continuum-regime Brownian coagulation at times longer than the characteristic coagulation time, a "self-preserving" asymptotic pdf shape was shown to extend to these bivariate populations, using the rescaled volume $v/\bar{v}(t)$ and rescaled area $a/\bar{a}(t)$ as "similarity" variables. This article considers the corresponding problem of coagulation in the "free-molecule" limit, relevant to the atmospheric pressure flame experiments of Xing et al. This combination of coagulation- and sintering-rate laws again leads to "self-preserving" rescaled jpdfs, explicitly time-independent for an isothermal environment, again dependent on a Damköhler-like number, $Dam_f$ (ratio of coagulation time to fusion time). While flames are more complex than our idealized simulations, our present pdfs and associated "mixed moments," capture important features of experimental results as one approaches the flame, especially evolution of a mean particle "shape factor," mean number of spherules per aggregate, and narrowness of the spread of spherule sizes. This agreement, coupled with the versatility of MC-methods for multistate variable particle population balances, encourages extensions leading to a versatile, tractable, formalism for the developing field of sol reaction engineering.*

## Introduction

### *Need for "multivariate" population balance models*

Particle production in gases, both deliberate and inadvertent, must be accurately predicted and controlled, motivating considerable theoretical and experimental research (Pratsinis, 1998; Rosner, 1997; Helble, 1998). In all of these applications it is rare that particle *size* alone is sufficient to characterize the "state" of a particle, since all relevant particle properties cannot generally be related to size (say, volume-equivalent diameter) alone. Moreover, the additional state variables of interest (such as shape and/or chemical composition) usually evolve dynamically in response to changing environmental conditions. Since a goal of *sol reaction engineering* is to predict the conditions necessary to efficiently produce particles of desired size, shape, and composition, simulation methods capable of dealing with multiple state variables are of current interest. Here, we deliberately focus attention on an instructive limiting case in which the chemical composition is fixed but the aerosol size and shape distributions respond to simultaneous Brownian coagulation and finite-rate "spheroidization." These are the circumstances studied in our recently reported counterflow laminar diffusion flame experiments on alumina nano-aggregates at particle volume fractions below 1 ppm (Xing et al., 1996, 1997, 1999). Indeed, the availability of these data serve to motivate the present MC-based simulations under "free-molecule" conditions, and suggest systematic extensions (as will be discussed later) to increase the realism and accuracy of such simulations. Systematic comparison of such simulations with well-defined measurements can also be used to extract physicochemical parameters (such as the activation energy for surface diffusion-controlled sinter-

Correspondence concerning this article should be addressed to D. E. Rosner.
Current address of S. Yu: Tsinghua Univ., Beijing 100084, China.

ing) that may be new or relatively inaccessible by more conventional "routes."

A potentially useful starting point, and one certainly capable of further development (see next section), is the "bivariate" model of Koch and Friedlander (1990), who chose particle *volume* and surface *area* as the particle state variables, and deliberately studied the simplest uncoupled rate laws governing the Brownian coagulation and area change of such particles. However, rather than assuming that particle morphology does not influence the collision frequency of particles of known volume, we illustrate the power of MC-based simulation methods for such multivariate population balance problems (see the next subsection) by introducing the fractal dimension $D_f$ as a "pre-specified" parameter. In the present context, this is clearly only an interim measure, since we expect that the operative fractal dimension will not be independent of the Damköhler number governing sintering (as will be discussed later)—moreover, in general the fractal dimension will be a *distributed* parameter (as is clear from some of the electron micrographs included in Xing et al., 1996, 1997). However, our position is that much can be learned from the body of results presented here, and semi-quantitative use of our locally self-preserving joint *pdf* results (and associated aerosol population "shape" parameters, including certain dimensionless "mixed moments" of particular physical interest (Rosner et al., 2000b)) may even be possible in certain time-dependent environments of practical interest. A later section of the article raises (and answers) the interesting question of whether our abovementioned "seeded" counterflow diffusion flames are among them, suggesting possible extensions to deal with the presently "missing couplings." Improved methods for predicting both the coagulation rates of nonspherical particles, and their mechanism-dependent sintering rates, will be the subject of future communications (Rosner, 2001). However, the essential point here is that these improved rate laws will be able to exploit the same MC-formalism illustrated in this article, and its continuum regime predecessor (Tandon and Rosner, 1999). Extensions to the more general case of a bi-variate aerosol evolution in response to a dynamically changing environment (including our laboratory flames in which the particles experience heating rates of the order of 40,000 K/s (Xing et al., 1997) will be briefly discussed later in this article and is the subject of current research (Rosner and Pyykonen, 2001). It is also possible that the availability of our present results, and selected extensions thereof, will be able to guide the as yet unprecedented development of more economical yet acceptably accurate "moment methods" (Cohen and Vaughn, 1971; Dobbins and Mulholland, 1984; Rosner and Tassopoulos, 1991; McGraw, 1997; Diemer, 1999; and Wright et al., 2001), now applicable in this "multi-variate" domain of *sol reaction engineering* (SRE).

### *Monte-Carlo based methods*

As in the cas of Monte-Carlo (MC) simulations of the molecular collision term in the Boltzmann equation of low density gas kinetic theory (Bird, 1994), it is possible to use a MC-based simulation (with appropriate use of a random number generator) of the local coagulation rate term, $(\partial n/\partial t)_{\text{coag.}}$ in the particle population balance IPDE (see, for example, Eq. 1 and Meakin (1987); Wu and Friedlander (1993); Tandon and Rosner (1999); Smith and Matsoukas (1998); Kruis et al. (2000)). For population balances in which particle *volume* is the only relevant state variable, the MC-method, while easy to program and implement, probably has no special numerical advantage over so-called "sectional" (finite-difference) methods. However, as the required number of particle *state variables* increases, MC-based methods will inevitably become computationally more attractive [see for example, Gooch and Hounslow (1996) and Tandon and Rosner (1999)], perhaps even compared to so-called "moment methods." [Interestingly enough, this same "particle-MC" philosophy applies to developing efficient computational methods to deal with *turbulent* single phase chemically reacting flows using so-called multi-variate "notional particle"-*pdf*-methods (Pope, 1985)]. In this article, building on the two-state variable precedent of Tandon and Rosner (1999), we explore MC-based simulations of the population balance for an aerosol coagulating in the free-molecule regime, simultaneously undergoing finite-rate coalescence ("spheroidization") in the asymptotic limit of times long compared to the characteristic coagulation time. Here, following Koch and Friedlander (1990), we define the "state" of a particle by its "wetted" surface *area a* as well as its *volume v* and adopt deliberately simple, uncoupled rate laws governing the interparticle collision frequency, and intra-particle "fusion" rate. By studying this class of "model" problems, we show that it is possible to gain an understanding of many important features of the joint *pdf* of volume and area in such a population, including its response to a Damköhler-like dimensionless parameter [constructed from the ratio of the characteristic *coagulation time* to the characteristic *sintering time* (see subsection on Bi-Variate "Self-Preserving Limit")].

### *Current (interim) treatment of the IPDE governing the time evolution of pdf(v,a)*

As will be discussed later, actual flame environments in which we have experimentally studied particle population evolution (Xing et al., 1996, 1997, 1999) are more complex than our present idealized simulations in several respects. In particular, not all particles at any given (residence) time can be characterized by the same fractal "dimension." Moreover, rather than a constant environment, and at times long compared to $t_{\text{coag}}$, from the vantage point of a particle, the rate of temperature change can be as large as 40,000 K/s! However, since there has been so little work on *bivariate* population balances, we are encouraged to deliberately idealize the situation studied here—starting with only a slight generalization of the rate laws first proposed by Koch and Friedlander (*loc cit*). Perhaps remarkably, our present dimensionless joint- and unconditional-*pdf*s, and associated "mixed" moments (Rosner et al., 2000b) will be shown to capture several important features of our recent experimental results—especially the evolution of a particle "shape factor" [calculated from thermophoretically acquired sample TEM images of alumina aggregate cross-section and perimeter (Xing et al., 1996, 1997)], the effective number of spherules per aggregate (*via* laser light scattering data; Xing et al., 1999), and narrowness of the spherule size distribution as one approaches the hot flame. This semi-quantitative agreement, coupled with the inherent versatility of such MC methods for multi-state vari-

able population balances with more accurate rate laws, encourages future extensions which will relax our most restrictive assumptions, including the "pre-specification" of an effective fractal dimension for the prevailing population (see also the subsection on $D_f$ Evolution). These extensions, currently under active study (Rosner, 2001), should be capable of providing: (a) realistic sintering rate parameter inferences from well-defined laboratory experiments of inorganic nano-aggregate *populations* restructuring in laminar flames, and lead to (b) a versatile, yet tractable, formalism for future design calculations in the developing *SRE*-field.

## Mathematical Model

### *Formulation of bivariate particle population balance equation*

Rather than immediately thinking of our population of suspended particles in terms of discrete "classes" (that is, the contents of size "bins" based on *volume*, and *area*), it is possible and conceptually useful to treat the individual particle size (say, *volume* $v$) and *surface area* $a$, as *continuous* variables, and derive a complete equation governing the evolution of a local number *distribution function* with respect to size and area: $n(v, a, \boldsymbol{x}, t)$ defined such that the expected number $dN$ of particles within the particle interval $v \pm dv/2$, $a \pm da/2$ and spatial volume $d\boldsymbol{x}$ centered at $\boldsymbol{x}$ can be written in terms of differentials

$$dN = n(v, a, \boldsymbol{x}, t)\; dv \cdot da \cdot d\boldsymbol{x} \tag{1}$$

0Thus, the function $n(v, a, \boldsymbol{x}, t)$ defined by Eq. 1 can be usefully regarded as a local particle "number density" but in a space $v$, $a$, $\boldsymbol{x}$ of independent variables that transcends physical space [see Ramkrishna (2000); Williams and Loyalka (1991); and Rosner (2000a)]. Alternatively, one can think of $n(v, a, \boldsymbol{x}, t)$ as the local, instantaneous value of $dN_p/dvda$ (that is, the contribution to the local particle number density: $N_p(\boldsymbol{x}, t)$ associated with particles in the size range: $v \pm dv/2$, and area range $a \pm da/2$) or view the ratio $n/N_p$ as the local normalized probability density function, *pdf* of the particle population with respect to $v$ and $a$. Of course, in practice, adequately defining the "state" of a particle may require more than two variables (here volume and area) and the formulation/MC solution procedures used below can be readily generalized to include such "multi-variate" cases (chemical composition, ...). For simplicity, we explicitly consider here only the case of a "dilute" aerosol—that is, one not only present in negligible *volume fraction*, but also present in a small *mass fraction* [for important aspects of the more general case, *cf*., Rosner and Park (1988)].

Reaction engineers are usually interested in applications where there are several contributions (convection, diffusion, phoresis, ...) to the velocity $\boldsymbol{v}_p$ of particles through physical space. Similarly, particles of size $v$ and area $a$ at $\boldsymbol{x}$,$t$ may have a "velocity in size space" (volumetric *growth rate*), written $\dot{v}(v, a, \boldsymbol{x}, t)$, and a "velocity through area space" written $\dot{a}(v, a, \boldsymbol{x}, t)$ (where the dependence on $\boldsymbol{x}$, $t$ is usually *via* local environmental conditions (that is, local state of the "carrier" gas mixture). Regarding particle "(net) source" terms, it is usually necessary to consider the consequences of particle-particle encounters which lead to "*coagulation*-coalescence," the possibility of particle "birth" *via nucleation* (subscript $N$) from the vapor, and the possibility of particle *breakup* (subscript $BU$).

If we now write an Eulerian particle population balance in the space of $\boldsymbol{x}$, $v$, and $a$, divide by the "volume" element $\Delta v \Delta a \Delta \boldsymbol{x}$, and pass to the limit of "vanishing" $\Delta v \Delta a \Delta \boldsymbol{x}$ we clearly obtain an equation of the Liouville form

$$\partial n/\partial t + \mathrm{div}(\boldsymbol{v}_p n) + \partial(\dot{v}n)/\partial v + \partial(\dot{a}n)/\partial a = \dot{n}_{\mathrm{coag}} + \dot{n}_N + \dot{n}_{BU} \tag{2}$$

where $\partial(\dot{v}n)/\partial v$ may be regarded as the "divergence" of the particle flux in particle size (*volume*) space, $\partial(\dot{a}n)\partial a$ may be regarded as the "divergence" of the particle flux in the particle *area* space, and where the net source terms associated with coagulation, nucleation, and/or breakup appear on the righthand side. To exploit this population balance Eq. 1, which can contain partial derivatives with respect to each of the indicated 6 independent variables, we must supply physically-based expressions for each of the important functions: $\boldsymbol{v}_p$, $\dot{v}$, $\dot{a}$, $\dot{n}_{\mathrm{coag}}$, $\dot{n}_N$, and $\dot{n}_{BU}$ appearing therein. Of course, these are application-specific, but, for most of the treatment below, we will explicitly neglect $\boldsymbol{v}_p$, $\dot{v}$, $\dot{n}_N$, and $\dot{n}_{BU}$, but address the simultaneous effects of $\dot{a}$, and $\dot{n}_{\mathrm{coag}}$. In considering the implications of our work for the description of restructuring nano-aggregates in a steady counterflow laminar diffusion flame, a situation for which we have acquired extensive data (Xing et al., 1996, 1997, 1999), we will have to also allow for nonzero $\boldsymbol{v}_p$, and, at least locally, $\dot{v}$ and $\dot{n}_N$, but these generalizations are best postponed (Rosner et al., 2000).

### *Brownian coagulation (free-molecule limit)*

If Brownian particle motion is the principal mechanism of binary (particle-particle) encounters, and only volume is used as the particle "state" variable, then, based on the work of Smoluchowski (1917), the net source $\dot{n}_{\mathrm{coag}}$ can be written as the difference between two integrals (Friedlander, 2000; Flagan and Seinfeld, 1988; Williams and Loyalka, 1991)

$$\dot{n}_{\mathrm{coag}} = (1/2) \cdot \int_0^v \beta(u, v)\, n(v-u, \ldots) \cdot n(u, \ldots)\, du - n(v, \ldots) \cdot \int_0^\infty \beta(u, v) \cdot n(u, \ldots)\, du \tag{3}$$

where, in the first term, the integration variable (particle volume) $u$ satisfies $0 \le u \le v$, $\beta(u, v)$ is the corresponding coagulation (binary) rate constant and we have assumed (see integrand of term 1) that volume (mass) is "conserved" in the collision-coalescence process. [Normally, these coagulation rate constants are inserted based on an independent microphysical submodel—that is, one normally solves the population balance with the function $\beta(u, v)$ *specified*. However, the "inverse" problem of *inferring* the function $\beta(u, v)$ from experimental observations of $n(v, \boldsymbol{x}, t)$ is feasible in principle (Wright and Ramkrishna, 1992), although infrequently done because this "ill-posed" problem requires rather special numerical treatment.] In the language of Randolph and Larson (1988), the first integral is the particle "birth" rate (B) and the second integral is the "death" rate (D).

The binary rate coefficient functions $\beta(u,v)$ appearing as a "kernel" in the IPDE (Eq. 2) *via* the net source term $\dot{n}_{\text{coag}}$ can be readily expressed in the *free-molecule limit* when ordinary Brownian motion is the mechanism that brings the particles of volumes $u, v$ together. In this limit, "hard-sphere" gas kinetic theory provides the coagulation rate-constant

$$\beta_{fm} = [3/(4\pi)]^{1/2} \cdot (6k_B T/\rho_p)^{1/2} \cdot [(1/u) + (1/v)]^{1/2} \cdot (u^{1/3} + v^{1/3})^{-2} \quad (4)$$

(Friedlander, 2000; Williams and Loyalka, 1991). Numerically important corrections to this rate constant expression are needed in many cases, especially when the colliding partners are no longer spherical (because in our present case, of slow coalescence (Koch and Friedlander, 1990; Tandon and Rosner, 1997; Oh and Sorensen, 1997) in the prevailing environment). An attack on this important problem, to provide $\beta(v, v', a, a')$ (where $u = v'$) for the suitably generalized form of Eq. 3 would take us too far afield here [see, for example, Rosner (2001) and the aggregate generation algorithm described in Filippov et al. (2000)], but we can at least move beyond the oversimplification that Eq. 4 remains applicable independent of the shapes (hence, areas) of the participating particles. Since the most prominent nonspherical class of shapes in the present problem is that of "fractal-like" aggregates, we can with some justification and very little computational complexity, generalize the last factor in Eq. 4 to read $(u^{1/D_f} + v^{1/D_f})^{\nu}$, where $\nu = \min(D_f, 2)$ (Flagan and Lunden, 1995), and the exponents now contain a population-averaged pre-specified "fractal dimension" $D_f$, which can be as low as *ca*. 1.7 for noncoalescing cluster-cluster aggregates. The prefactor to $(6\ k_B T/\rho_p)^{1/2}$ is then written: $[3/(4\pi)]^{1/6} \cdot (v_1)^{(2/3)-(\nu/D_f)}$]. We postpone to a later section a discussion of the meaningful "assignment" of $D_f$, and its possible "linkage" to the Damköhler number governing the fusion rate process. In most numerical illustrations below we will emphasize the limiting cases of $D_f = 3$ (uniformly dense spheres) and $D_f =$ 1.8 (cluster-cluster aggregates in the absence of sintering), although some of our graphs will show results for intermediate $D_f$-values that have been observed in practice (such as $D_f =$ 2.2 and 2.5).

### *Spheroidization ("fusion") kinetics*

The fourth term, $\partial(\dot{a}n)/\partial a$, on the lefthand side of Eq. 2 is the result of particles undergoing surface-energy driven "spheroidization" (restructuring) and a mechanistically realistic sintering rate law, providing the function $\dot{a}(v, a, t)$ for an individual particle in the population, must be specified. Here, the time variable $t$ usually enters *implicitly* through the instantaneous temperature of the particle's environment. Based on the long-time sintering behavior of two spherules of radius $R_1$, Koch and Friedlander (1990) suggested the following linearized expression for the rate of surface area reduction

$$\dot{a} \equiv da/dt = -[a - a_{\text{final}}(v)]/t_f, \quad (5)$$

where $a_{\text{final}}$ is the surface area of the fully compacted sphere of the same volume. Not surprisingly, the relaxation time $t_f$ appearing in Eq. 5 is mechanism-specific. Thus, for spheroidization as a result of *surface diffusion* (Mullins, 1995).

$$t_f = [k_B T \cdot (R_1)^4] / [24 D_s v_m \sigma \delta] \quad (6)$$

whereas, for *bulk diffusion* (Friedlander, 2000)

$$t_f = [k_B T \cdot (R_1)^3] / [12 D_v v_m \sigma] \quad (7)$$

Here $k_B$ is the Boltzmann constant, and $D_s$ and $D_v$, are, respectively, the surface- and volume-diffusion coefficients (with units $m^2/s$), $v_m$ is the effective molecular volume in the condensed phase, and factor $\delta$ is a surface diffusion layer thickness, approximately equal to $3 \cdot (6 v_m/\pi)^{1/3}$. Lastly, for *viscous flow* sintering (*cf*., Friedlander, 2000; Ulrich and Subramanian, 1977; Helble and Sarofim, 1989), the characteristic time of fusion/sintering $t_f$ is found to be

$$t_f = \mu R_1/\sigma \quad (8)$$

where $\mu$ is the spherule Newtonian viscosity and $\sigma$ is the particle surface energy. Following Koch and Friedlander (1990), in the simplest simulations the characteristic time $t_f$ is considered to be time-independent, even though (as will be illustrated later) these laws can plausibly be applied to restructuring aggregates of more complex morphology with $d_{1,\text{eff}} = 2R_{1,\text{eff}}$ taken to be $d_{1,\text{eff}} = 6v/a$. In this connection, the 4th power sensitivity of $t_f$ to effective spherule diameter for the surface diffusion mechanism is noteworthy, in part accounting for the "terminal" nano-spherule sizes normally seen in flame-grown oxide fractal aggregates (Xing and Rosner, 1999).

It is appropriate to comment here that aggregate restructuring, in general, also results in an increase in fractal dimension (Tandon and Rosner, 1996; Xing et al., 1997, 1999; Yang and Biswas, 1997)—a fact which will have to be incorporated in a self-consistent manner in future applications of our MC-method (see later section and Rosner et al., 2000). Moreover, our "pseudo-homogeneous" methods applied to large aggregates with $D_f > 2$ (Tandon and Rosner, 1996) already reveal the need for aggregate area reduction rate-laws more complex than the two-sphere sintering behavior mentioned above. Relaxing these oversimplifying assumptions (work in progress) is likely to preclude the existence of a "self-preserving" solution even with formally pre-specified $D_f$ (see next subsection). However, even in such situations, our present simulation methods will remain valid for predicting the evolution of aggregating-restructuring populations. Furthermore, Monte-Carlo methods are versatile enough to handle rather complex couplings between the coagulation and fusion terms in solving the population balance equation.

### *Bivariate "self-preserving" limit*

For a suspended population with number distribution function $n(v, a, t)$ at time $t$, the total particle *number density*, $N_p$, and volume fraction, $\phi_p$, are clearly

$$N_p = \int_0^\infty \int_0^\infty n(v, a; t) \cdot dv \cdot da \quad (9)$$

and

$$\phi_p = \int_0^\infty \int_0^\infty (v) \cdot n(v, a; t) \cdot dv \cdot da \tag{10}$$

and the ratio of $\phi_p$ and $N_p$ provides one important average "aggregate" volume $\bar{v}$ in the population. Likewise, an average aggregate *area* can be defined by

$$\bar{a} \equiv (1/N_p) \cdot \int_0^\infty \int_0^\infty (a) \cdot n(v, a; t) \cdot dv \cdot da \tag{11}$$

so that the *total surface area per unit volume*, $a'''$, can be written: $N_p \bar{a}$.

Anticipating simplifications associated with the long time asymptote ($t/t_{\text{coag}} \gg 1$), we now define the "rescaled" (similarity-transformed, dimensionless) particle state variables as

$$\eta_1 \equiv v/\bar{v} \qquad \eta_2 \equiv a/\bar{a} \tag{12}$$

and define the corresponding dimensionless *pdf*s

$$\Psi_{12} \equiv \bar{v} \cdot \bar{a} \cdot n(v, a; t)/N_p \tag{13a}$$

$$\Psi_1 \equiv (\bar{v}/N_p) \cdot \int_0^\infty n(v, a; t) \cdot da \tag{13b}$$

$$\Psi_2 \equiv (\bar{a}/N_p) \cdot \int_0^\infty n(v, a; t) \cdot dv \tag{13c}$$

where $\Psi_{12}$ is clearly the dimensionless *joint* pdf $n(v, a, t)$ between rescaled particle volume and area, $\Psi_1$ is the "unconditional" distribution function with respect to scaled volume (irrespective of area), and $\Psi_2$ is the "unconditional" distribution function with respect to scaled area (irrespective of volume). The behavior of the bivariate distribution function, here economically described *via* $\Psi_{12}(\eta_1, \eta_2)$ is needed in many applications (see next subsection and Rosner et al., 1999, 2000b), and numerical simulation results, and will also be useful in developing "moment-method" approximate solutions to the population balance equation with two "internal" variables (such as size, surface area; Wright et al., 2001).

Apart from the prespecified morphological parameter $D_f$, [this is clearly an instructive interim measure (also exploited in Tsantilis and Pratsinis, 2000) to be relaxed in our future work; see later section], the effective fractal dimension of the nonspherical particle population, our solutions will also depend on a dimensionless parameter specifying the relative rates of the coagulation and fusion (sintering) processes. This is conveniently chosen to be the characteristic time ratio: $t_{\text{coag}}/t_{\text{fusion}}$, which plays the role of a Damköhler number familiar to chemical reaction engineers (Rosner, 2000a). For this reason, we introduce the dimensionless parameter $(Dam)_f = t_{\text{coag}}/t_{\text{fusion}}$, where the fusion time $t_f$ has been defined above, and, based on the abovementioned $\beta(u, v; D_f)$ expression, we choose

$$t_{\text{coag}} = (K_{fm} \cdot N_p)^{-1} \tag{14a}$$

where

$$K_{fm} \equiv [3/(4\pi)]^{1/6} \cdot (6k_B T/\rho_p)^{1/2} \cdot (v_1)^{(1/6)} \tag{14b}$$

While it is straightforward to prove the existence of "self-preserving" behavior with respect to scaled *volume*, for our choice of rate laws governing coagulation frequency (Eq. 4) and surface *area* reduction (Eq. 5) self-preserving behavior with respect to *area* will here be "empirically" established by comparing the solution (see Results and Discussion section) at rather different dimensionless times (that is, Monte-Carlo time steps) subject to the condition that a sufficiently large number of coagulating particles remain (*cf*., Smith and Matsoukas, 1998). More realistic coagulation and sintering laws will, in general, preclude the existence of "self-preserving" solutions, but it is noteworthy that our MC-based simulation methods will still be able to predict aggregate population dynamics in these more realistic cases.

Using the abovementioned (deliberately "idealized") rate laws, and the MC simulation methods described in the next section, in the so-called "self preserving" or long-time limit we have numerically constructed the abovementioned functions $\Psi_{12}(\eta_1, \eta_2; (\text{Dam})_f, D_f)$, $\Psi_1(\eta_1, D_f)$, and $\Psi_2(\eta_2; (\text{Dam})_f, D_f)$, as well as a number of important quantities derived. Most of these results will be collected and discussed later.

### *Dimensionless "mixed moments" of interest*

We will also be interested in several dimensionless "mixed" moments $\mu_{kl}$ of the *jpdf* $\Psi_{12}(\eta_1, \eta_2)$, where:

$$\mu_{kl} \equiv \int_0^\infty \int_0^\infty (\eta_1)^k \cdot (\eta_2)^l \cdot \Psi_{12}(\eta_1, \eta_2) \cdot d\eta_1 \cdot d\eta_2 \tag{15}$$

and the indicated exponents $k$, $l$ on the righthand side need not be positive or integers. Of course, several of these ($\mu_{00}$, $\mu_{10}$, and $\mu_{01}$) must be *unity* as a result of the definitions above, which can serve as a check on the accuracy/precision of our numerical methods.

Extending our earlier work on total deposition rates in the "univariate" case (Rosner, 1989; Rosner and Tassopoulos, 1989; Rosner and Khalil, 1999) other dimensionless "mixed" moments have a particular physical significance (Rosner et al., 2000), an example being the particular moment: $\mu_{1,-2/3}$. This can be regarded as a first approximation to the dimensionless *ratio* $\mathfrak{R}$:

$$\mathfrak{R} \equiv \frac{\begin{pmatrix}\text{actual total mass deposition rate}\\ \text{from the aerosol population}\end{pmatrix}}{\begin{pmatrix}\text{reference deposition rate (in same environment)}\\ \text{if all particles had volume } \bar{v} \text{ and area } \bar{a}\end{pmatrix}} \tag{16}$$

for the case of isothermal *convective-diffusion mass transfer* in the (aerosol-) limit of very large Schmidt number, when the particles are in the free-molecule regime ($Kn_p \gg 1$). This follows from the approximate dependencies: Brownian diffusivity $\sim a^{-1}$ and mass deposition rate $\sim vD^{2/3}\, n\, dv\, da$.

Accurate values of the "mixed" moments will also be of special interest because there is an important class of approximate methods for solving population-balance problems which proceed by deriving/solving a closed set of coupled differential equations governing selected "lower moments" some of which may be of greater physical interest than the "recon-

structed" *pdf* itself (Hulburt and Katz, 1964; Cohen and Vaughn, 1971; Dobbins and Mulholland, 1984; Frenklach and Harris, 1984; Rosner and Tassopoulos, 1991; McGraw, 1997; Diemer, 1999; Wright et al., 2001). Thus, our present MC results, which include the $\mu_{kl}$- "surfaces" [on the $k$, $l$ "plane" (as will be shown in Figures 10 and 11)] will be valuable in reliably extending such methods into the multi-variate domain (Rosner et al., 2000b).

## Monte-Carlo (MC-) Simulation Method

### *MC simulation and required computer resources*

The rate of change of an aggregate distribution function by the simultaneous action of Brownian coagulation and intraparticle sintering is represented by Eq. 2 (such as Koch and Friedlander, 1990). This is seen to be a nonlinear integropartial differential equation, which, for realistic collision "kernels" and even simple sintering rate laws, must be solved numerically. Thus far, both "sectional" methods (Xiong and Pratsinis, 1993) and Monte-Carlo methods (Wu and Friedlander, 1993; Tandon and Rosner, 1999; Gooch and Hounslow, 1996) have been employed for this purpose. In "sectional" models, in which the particle state variable space is conveniently discretized, the calculation of intersectional collision rates is very demanding of CPU time (Wu and Flagan, 1988; Landgrebe and Pratsinis, 1990; and Lu, 1994), even for the case of only one particle state variable. Thus, with current computer resources, Yu and Kennedy (1997) could only use an approximate method to calculate sectional collision rates in their recent one-variable aerosol dynamic studies of chromium oxide particle evolution in laminar flames. Since the calculation of two-variable intersectional collision rates is even more demanding (Xiong and Pratsinis, 1993), it is reasonable and quite tractable to employ a Monte-Carlo simulation method in the present two-state variable study (and future *tri-variate* extensions). In the next section we will show that the MC method can yield the same accuracy as the more familiar sectional method for the univariate self-preserving aerosol coagulation case [see, also, Smith and Matsoukas (1998); Figure 6 in that article].

### *Treatment of Brownian coagulation of fractal aggregates in the free-molecule regime*

There are several variants of the Monte Carlo method to solve the aggregate coagulation (Meakin, 1987; Wu and Friedlander, 1993; Smith and Matsoukas, 1998; Tandon and Rosner, 1999). In this study, the MC method used was similar to that of Meakin, and Smith and Matsoukas (*loc cit*), but generalized to the 2-state variable case by Tandon and Rosner (1999).

In this MC algorithm, 10,000 particles are considered, each initially of unit volume and unit area. At each time, two particles $i$ and $j$ are randomly selected from the particle list and the collision frequency function $\beta(v_i, v_j)$ and $\beta_{\max}$ are evaluated. $\beta_{\max}$ is the maximum value of collision frequency function for any pair of particles on the list at this time. A random number between 0 and 1 is then generated and compared with the collision frequency ratio $\beta(v_i, v_j)/\beta_{\max}$. If the chosen number is smaller than the collision frequency ratio, the two particles $i$ and $j$ are coagulated to form a particle with volume $v_i + v_j$ and area $a_i + a_j$; otherwise, the two chosen particles $i$ and $j$ are returned to the list and we rechoose two particles and a new random number. When a successful collision takes place, the coagulated particle is replaced on one site of the original $i$ or $j$ and one vacant site is created. In such a case, one particle is randomly copied from the current list to the vacant site. These procedures are shown in Figure 1, where the time intervals are *not* of equal length, increasing in proportion to $[1-(1/N)]^{-\kappa}$, where $N$ is the number of particles initially considered, and $\kappa$ is the number of coagulation events (Smith and Matsoukas, *loc. cit.* Eq. 24). Each vertical column represents the 10,000 particle list, but at different times. Two successive columns represent successive collision events and so on.

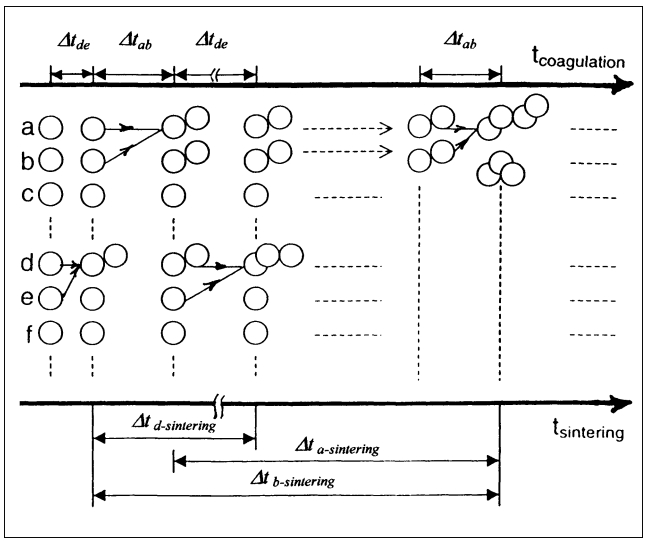


**Figure 1. Present Monte-Carlo simulation technique for a population of particles which simultaneously coagulate and spheroidize at finite rates.**

(See also Tandon and Rosner, 1999). Time intervals along top are those between coagulation events, and are inversely proportional to the corresponding $\beta$-values.

MC simulations are carried over a large number of time steps to reach the now familiar (Tandon and Rosner, 1999; Wright et al., 2000) asymptotic *bi-variate* "self-preserving" distributions. Indeed, the minimum number of time steps to reach a self-preserving distribution not only depends on the number of particles in the list, but also on the initial particle volume- and area- distributions in the particle list, and fractal dimension. For example, in a 10,000 "monodispersed" particle list with a fractal dimension of 3, the minimum number of steps needed is about 300,000 [larger than the corresponding case in the continuum regime (Tandon and Rosner, 1999; Vemury et al., 1994)]. On the other hand, for a particle list with given particle number, initial distribution and fractal dimension, the number of MC simulation steps has an upper limit due to the demands of numerical accuracy. Of course, the mean diameter of the particle list increases with an increase of the MC simulation step number. When mean diameter increases to certain value, the particle number needed for the corresponding self-preserving distribution will exceed the initial particle number in the list. For the previous example, the maximum number of steps is taken to be 500,000. Systematic studies of the times to achieve *self-preservation with*

*respect to area* are beyond the scope of the present work, but will be dealt with elsewhere (Wright et al., 2000; Rosner and Yu, 2000).

### *Treatment of sintering kinetics*

A sintering calculation is embedded in the MC-based coagulation simulation (see Figure 1 and Eq. 5). In the simplest cases, the separable ODE (Eq. 5) for the area evolution of an individual particle of fixed volume $v$ can be integrated analytically, accounting for the real-time interval between successive coagulation events. This result can be applied after the particle is formed by coagulation until the time it is selected to coagulate with another particle. During this interval, one or more coagulation events with other particles might take place. Thus, rather than calculating the area reduction for all particles at each step, we need only calculate the sintering for the selected particles from *their* last coagulation event to the current time level. This was one important technique to save CPU time in the present MC simulations, thereby permitting the use of larger ensembles (see below).

### *Averaging procedure*

An "ensemble" of simulations ("realizations") is needed to average the results in order to reduce the inevitable statistical noise in such MC simulations. More efficient MC simulation algorithms make possible larger ensembles. For example, averaging over 25 simulations for the case in the previous subsection required only 35–40 min on a Yale Engineering Hewlett Packard 9000 workstation. Actually, most of the results presented here (next section) used averaging over more than 100 realizations, which accounts in part for the "noise reduction" when compared with the continuum regime results of Tandon and Rosner (1999).

## Results and Discussion

### *Unconditional distributions wrt scaled particle volume $v/\bar{v}$ and $v_1/\bar{v}_1$*

Our ensemble-averaged MC-results for the unconditional self-preserving distributions with respect to dimensionless particle *volume*; for $D_f = 3$, are collected in Figures 2a and 2b. Subject to the simplified rate laws discussed earlier, these results should be independent of $(\mathrm{Dam})_f$ and agree with previous "univariate" results for the dimensionless *volume* distribution. As a (partial) confirmation of the success of our present MC simulation method, also shown in Figure 2, is a comparison with the earlier univariate "sectional" method $D_f = 3$ calculations of Vemury et al. (1995). Note that departures of volume-weighted PSD from Gaussian shape on these coordinates (Figure 2b) reveal modest but systematic departures from "log-normality." These departures play an important role for phenomena dependent on volume moments higher than 2 (such as, inertial deposition and laser light scattering, …).

For the important limiting case $D_f = 1.8$ [our numerical results ($\Psi_1$ and $\eta_1 \cdot \Psi_1$) for $D_f = 2$ were also in excellent agreement with those of Vemury et al. (1995) (the lowest $D_f$-value they considered)], Figure 3a shows our corresponding unconditional self-preserving distributions with respect to dimensionless particle *volume*. Also shown, for comparison, is the

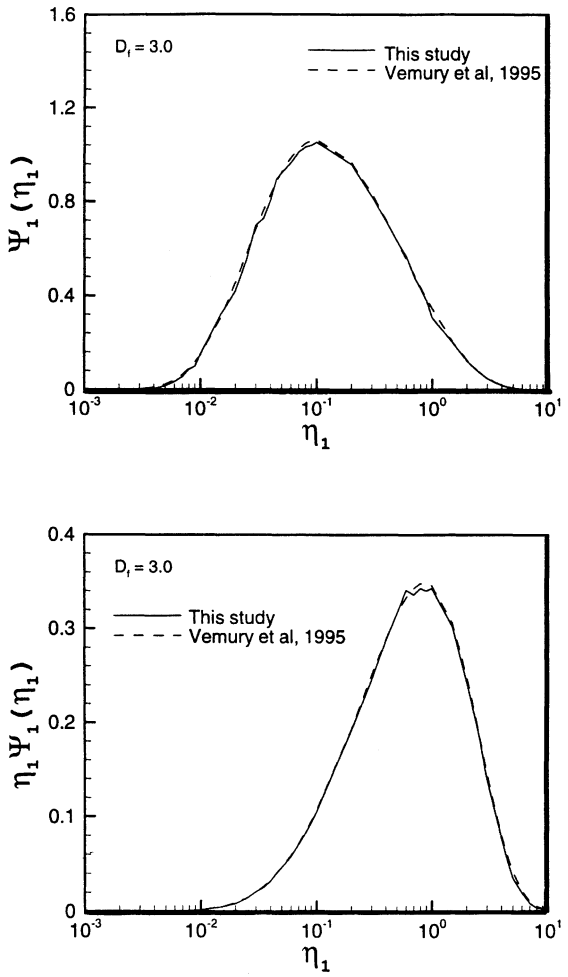


**Figure 2. Unconditional self-preserving distributions with respect to dimensionless particle volume; $D_f = 3$, showing comparison of present MC-results with the univariate "sectional" method calculation of Vemury and Pratsinis (1995).**

Departure of volume-weighted PSD from Gaussian shape reveals systematic departure from "log-normality."

unconditional *pdf* of $N_{\mathrm{eff}}$, the effective number of spherules per aggregate for the case $\mathrm{Dam}_f = 10^{-5}$ ("slow" fusion). *In general* these two *pdf*s are different, because in the present model not all "spherules" necessarily have the same size. However, in this Damköhler number limit these two *pdf*s are seen to be rather close because of the (often reported) narrowness of the effective spherule size distribution. Indeed, Figure 3a also shows the unconditional self-preserving distribution of dimensionless effective *spherule volume*, again for $D_f = 1.8$ and $\mathrm{Dam}_f = 10^{-5}$. [Recall that, in the present model, effective spherule volume is computed from the effective spherule diameter $6v/a$, and (in Figures 3a and 3b) is nondimensionalized by the number-*mean* spherule volume.]

Figure 3b shows the corresponding unconditional self-preserving distributions with respect to dimensionless *volume* for $D_f = 1.8$ when $\mathrm{Dam}_f = 1$("rapid" fusion). Also shown is the nearly identical *pdf* of effective "spherule" volume, again

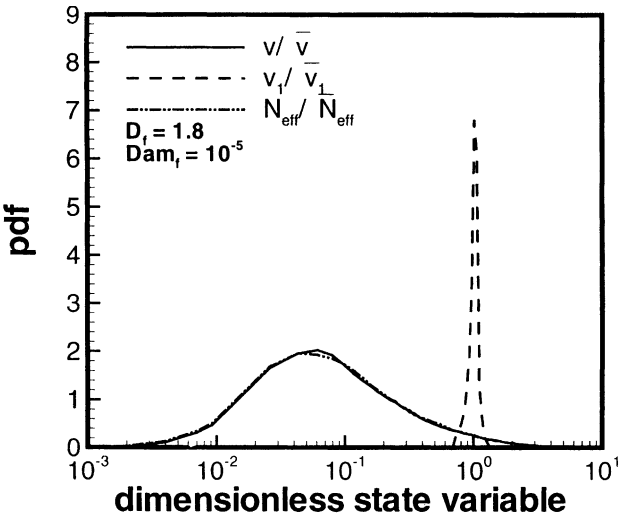


**Figure 3a. Unconditional self-preserving distribution with respect to dimensionless particle volume; $D_f = 1.8$ when $Dam_f = 10^{-5}$.**

Shown, for comparison, is the (nearly identical) unconditional *pdf* of $N_{\text{eff}}$, the effective number of spherules per aggregate, and the inferred (quite narrow) *pdf* of effective spherule size, $v_{1,\text{eff}}$ (where effective spherule volume is computed from the effective spherule diameter $6v/a$), and is nondimensionalized by the *mean* spherule volume.

computed from the effective spherule diameter $6v/a$ and nondimensionalized by the *mean* spherule volume. In this Damköhler number limit nearly all particles are comprised of one "spherule," as is clear from the narrow *pdf* of $N_{\text{eff}}$ (ratioed to the mean value of $N_{\text{eff}}$, also shown).

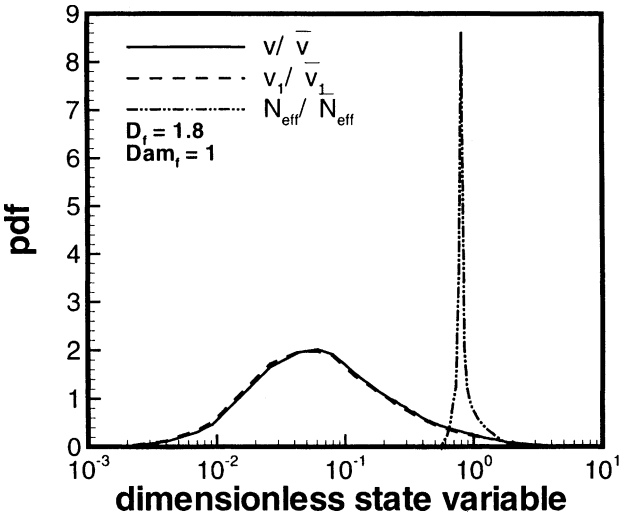


**Figure 3b. Unconditional self-preserving distributions with respect to dimensionless *spherule volume* for $D_f = 1.8$ when $Dam_f = 1$ (rapid fusion).**

Also shown is the (nearly identical) *pdf* of effective "spherule" volume computed from the effective spherule diameter $6v/a$ and nondimensionalized by the *mean* spherule volume. In this limit nearly all particles are comprised of one "spherule."

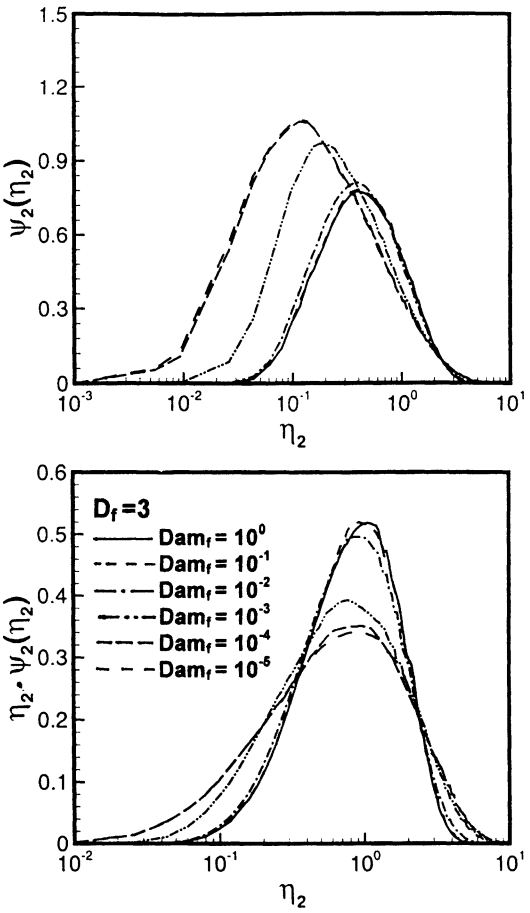


**Figure 4. Unconditional self-preserving distributions with respect to dimensionless particle *area* predicted by present MC method for $D_f = 3$, showing dependence on Damköhler number, $Dam_f$ for fusion (sintering).**

### *Unconditional distributions wrt scaled particle surface area: $\Psi_2$ and $\eta_2 \cdot \Psi_2$*

Unconditional self-preserving distributions with respect to dimensionless particle *area* $\eta_2$, formally predicted by the present MC-method for $D_f = 3$ are collected in Figures 4a and 4b. Note the systematic dependence on the Damköhler number, $\text{Dam}_f$ for fusion (sintering), with slow fusion corresponding to a larger number of particles of small surface area. Corresponding results for the important limiting case $D_f = 1.8$ are shown in Figures 5a and 5b. The MC-predicted Damköhler number dependence of the effective *spreads*, $\sigma_{g,a}$, of these unconditional *pdf*s with respect to *area* are shown in Figure 8 over a range of pre-specified fractal dimensions, $D_f$, between 1.8 and 3.

### *Joint pdf of particle volume and surface area*

A convenient way to display our ensemble-averaged MC-results for the *jpdf*: $\Psi_{12}[\eta_1, \eta_2; (\text{Dam})_f, D_f]$ is to show $\Psi_{12}$-"cuts" at various values of the scaled volume $\eta_1 = v/\bar{v}$. Figure 6 shows such "conditional" self-preserving distributions (with respect to dimensionless particle *area*, "given" volume) for $D_f = 3$, with Panel a corresponding to $\text{Dam}_f = 10^{-5}$ ("slow"

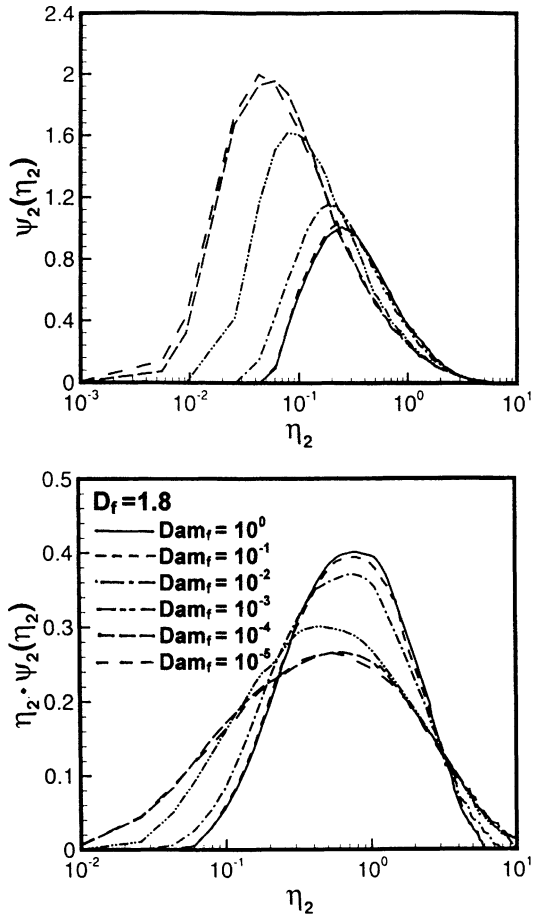


**Figure 5. Unconditional self-preserving distributions with respect to dimensionless particle *area* predicted by present MC method for $D_f = 1.8$, showing dependence on Damköhler number $Dam_f$ for fusion (sintering).**

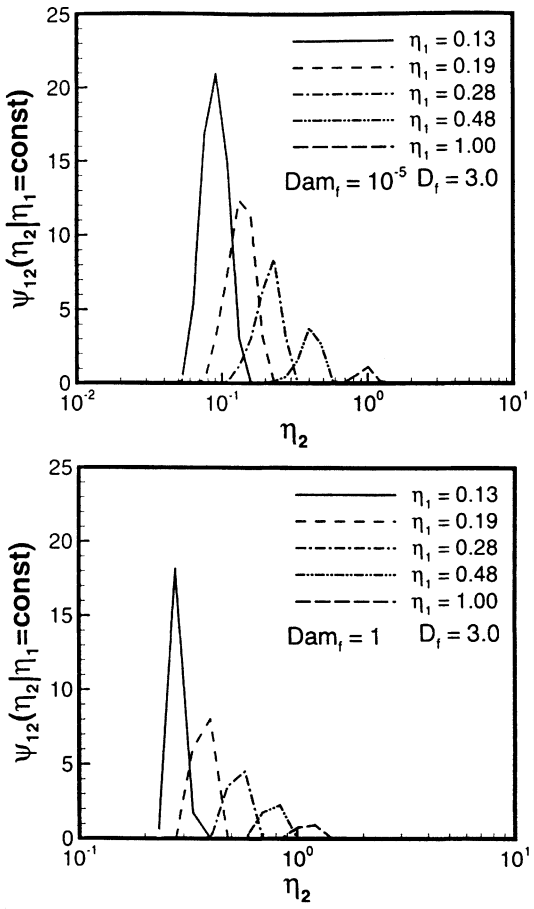


**Figure 6. Conditional self-preserving distributions with respect to dimensionless particle *area*, "given" volume, as predicted by present MC method for $D_f = 3$.**

Cases shown: (a) $Dam_f = 10^{-5}$; and (b) $Dam_f = 1$.

fusion) and Panel b corresponding to $Dam_f = 1$ ("rapid" fusion). Analogous results for the important limiting case: $D_f = 1.8$ are shown in Figures 7a and 7b. It is interesting to note how narrow each of these *conditional* distributions is (*cf.* $\Psi_2$ (Eq. 13c).

### *Dimensionless "moments" wrt scaled volume and area: and dependence on $(Dam)_f$, and $D_f$*

Ensemble-averaged MC-predictions of contours of constant dimensionless "mixed moment" on the $k$, $l$ plane are collected (as will be shown in Figure 10) over a range of Damköhler numbers for the pre-specified fractal dimension $D_f = 3$. Corresponding "surfaces" for the limiting case $D_f = 1.8$ are collected as will be shown in Figure 11. In both sets of figures, values of $Dam)_f$ range from $10^{-5}$ (lower left) to $10^0$ (upper right) in multiples of 10. Note that an increased relative fusion rate introduces a $\mu_{kl}$ dependence along the direction of slope $-1$ on the $k$, $l$ plane (*cf.* Eq. 15). Also, note that, as required, the values of $\mu_{00}$, $\mu_{10}$, and $\mu_{01}$ are each unity (actually, to better than 0.02%). Of particular interest for estimating $Sc \gg 1$ Brownian deposition from such particle populations is the particular moment $\mu_{1,-2/3}$ (as discussed earlier and Rosner et al., 2000b). Figure 12 will show the MC-predicted Damköhler number dependence of $\mu_{1,-2/3}$ over a range of pre-specified fractal dimensions $D_f$ between 1.8 and 3.

### *Dimensionless area ratio: $\bar{a}/a_{min}(\bar{v})$*

An important "shape factor" for the restructuring "bivariate" aerosol population is the dimensionless ratio: $\bar{a}/a_{\min}(\bar{v})$, readily computed from our ensemble-averaged MC-results for $\Psi_{12}[\eta_1, \eta_2; (Dam)_f, D_f]$ and the definitions of $a$ and $v$ (as discussed earlier). Figure 9 shows the Damköhler number dependence of this dimensionless mean area for the population over a range of pre-specified fractal dimensions $D_f$, between 1.8 and 3. As will be briefly discussed, this parameter can also be taken as a measure of $(\bar{N}_{\text{eff}})^{1/3}$, where $N_{\text{eff}}$ is the mean number of effective spherules per aggregate in the population. (These two quantities can be shown to differ only by the interesting factor: $(\mu_{-2,+3})^{-1/3}$.) We note that for fractal-like objects with $D_f < 2$, $pdf(N)$ and $N_{\text{eff}}$ are experimentally accessible *via* angular laser light scattering measurements (Xing et al., 1999).

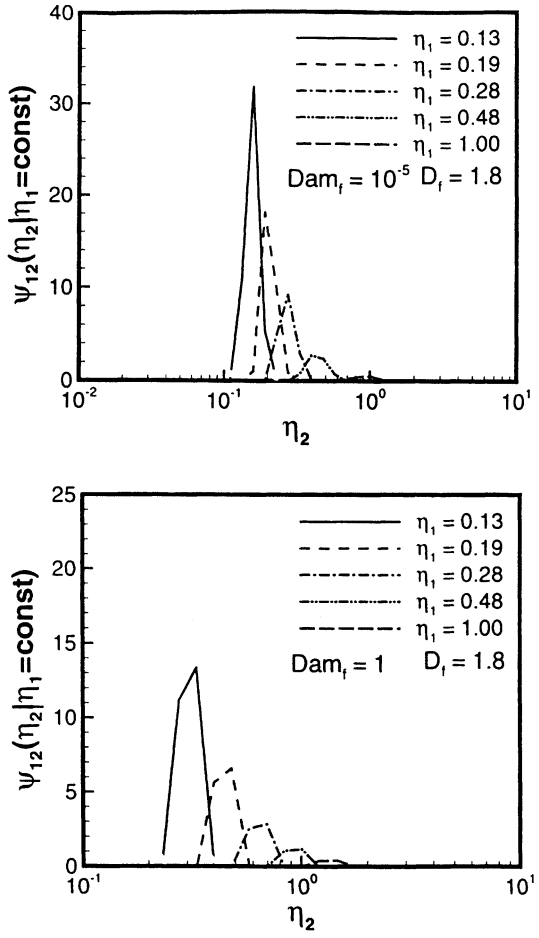


**Figure 7. Conditional self-preserving distributions with respect to dimensionless particle *area*, " given" volume, as predicted by present MC method for $D_f = 1.8$.**

Cases shown: (a) $Dam_f = 10^{-5}$; (b) $Dam_f = 1$.

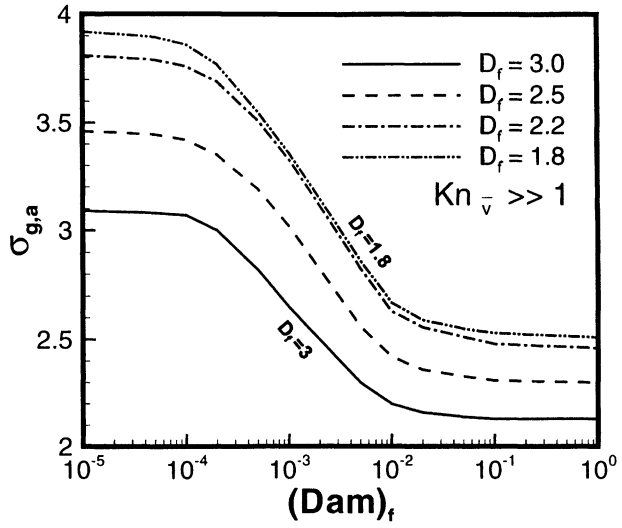


**Figure 8. Damköhler number dependence of the effective *spreads*, $\sigma_{g,a}$, of the unconditional *pdf* with respect to *area*.**

MC predictions over range of pre-specified fractal dimension $D_f$ between 1.8 and 3.

### *MC-results for variable fusion time*

The previous results were formally predicted under the simplest assumption for the fusion time, $t_f$, *viz*. that it remains constant. However, the MC-method facilitates allowing $t_f$ to vary with the effective spherule size $d_{1,\text{eff}} = 6v/a$ according to the prevailing coalescence mechanism. The systematic effects of sintering rate law (*cf. const.* $t_f$, viscous flow $t_f$, and surface-diffusion $t_f$) on the MC-predicted unconditional *pdf* with respect to scaled surface *area* for a population with $D_f = 1.8$ are displayed in Figure 13. The extreme cases shown are: (a) $(\text{Dam})_{f,t=0} = 10^{-5}$ and (b) $(\text{Dam})_{f,t=0} = 1$. It is interesting to note that the effects on $\eta_2 \cdot \Psi_2$ are less prominent than on $\Psi_2$ itself; moreover, the effects become more noticeable as $\text{Dam}_f$ increases.

## Preliminary Discussion of Relation to CDF Experimental Data

It is tempting to apply, to the fullest extent possible, information derived from the present mathematical model of simultaneous coagulation and sintering to available experimental (TPS/TEM- and LLS-) data on alumina nanoparticle evolution in our steady, atmospheric pressure laminar counterflow diffusion flames (Xing et al., 1996, 1997, 1999). At first sight, the situations appear too different, with our present simulations describing a transient, spatially homogeneous aerosol in a time-invariant environment. However, when it is realized that, downstream of the "particle inception" plane, axial Brownian diffusion plays little role under our experimental conditions, then $t$ in the present analysis can be regarded as a Lagrangian variable—that is, *elapsed time* as recorded by the population of particles moving through the

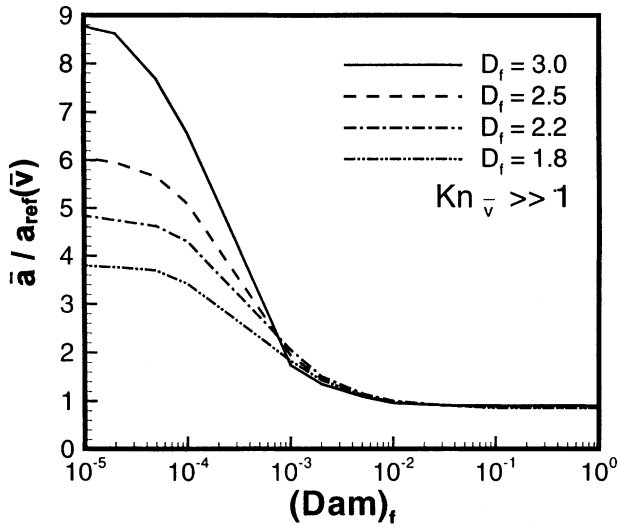


**Figure 9. Damköhler number dependence of the dimensionless mean area of population.**

MC predictions over a range of pre-specified fractal dimensions $D_f$ between 1.8 and 3.

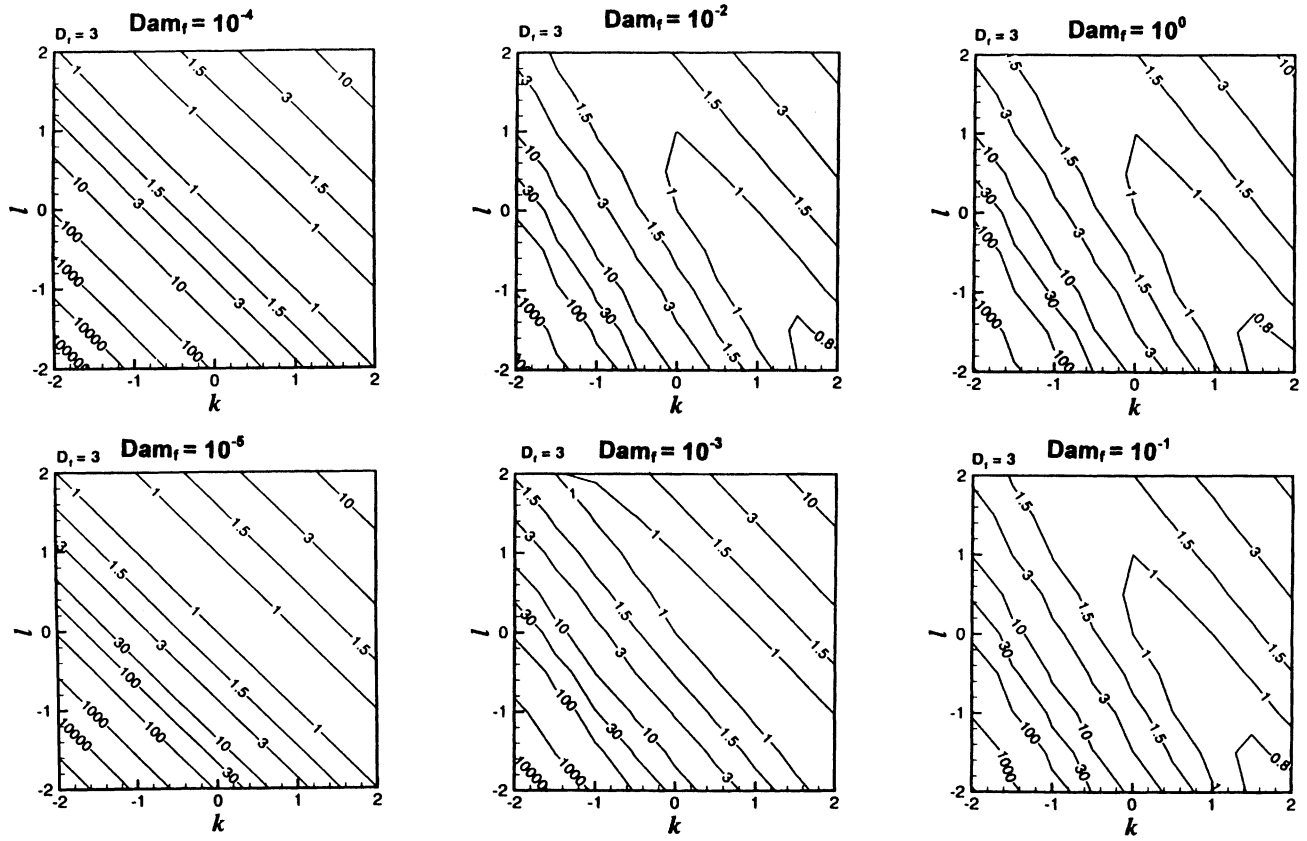


**Figure 10. Contours of constant dimensionless "mixed moments" on the *k*,*l* plane.**

Ensemble-averaged MC-predictions over a range of Damköhler numbers for pre-specified fractal dimension $D_f = 3$; Values of $(Dam)_f$ (indicated on top of each panel) range from $10^{-5}$ (lower left) to 1 (upper right), in multiples of 10. (See also Rosner et al., 2000b).

axial coordinate $z$ in space, as a result of gas convection, $v_{g,z}(z)$ and *axial thermophoresis* $v_{p,T;z}(z)$ (Gomez and Rosner, 1993). [We exploit the simplification that the local thermophoretic velocity, $v_{p,T;z}(z)$, will be insensitive to particle size and *morphology* (Rosner et al., 1991). In effect, neglect of Brownian diffusion, and insensitivity of thermophoretic velocity to (volume-equivalent) size were already (implicitly) exploited in the pioneering silane-seeded CDF paper by Zacharaiah and Semerjian (1989). However, these authors did not track morphological changes in detail, whether *via* TPS/TEM or LLS.] Then, apart from accuracy of the coagulation- and sintering- *rate laws* underlying our simulations, an immediate question arises as to whether, again from the vantage point of the particles, environmental conditions change too rapidly to permit *local* application of our present "self-preserving" results. This crucial point, and related questions, are taken up in the sections which follow.

### *Characteristic times and time to achieve "self-preservation"*

Reduction of the present population balance to an IPDE with solutions of the compact "self-preserving" form: $\Psi_{12}[\eta_1, \eta_2; (\mathrm{Dam})_f, D_f]$ requires that the elapsed dimensionless time exceed a "relaxation" time written $(\Delta t)_{\mathrm{SP}}/t_{\mathrm{coag}} = fct.\,[(\mathrm{Dam})_f, D_f]$, where the indicated function can now be explored numerically, using the present MC formalism (Yu et al., 2001) [Vemury et al., 1994) have provided values of $fct(\infty, 3)$ for initially log-normal particle populations]. Local quantitative application of our present results to the abovementioned flame environment would therefore require that the characteristic times associated with the flame environment (Xing et al., 1996, 1997, 1999) be small compared to $(\Delta t)_{\mathrm{SP}}$. We show below that this necessary condition is *not* met, so that a "full" simulation of the bivariate aerosol population dynamics (*via* Eq. 2) will evidently be required. Fortunately, an MC-simulation of the coagulation term remains attractive, by analogy to the use of such simulation methods in gas kinetic theory (Bird, 1994; Papadopoulos and Rosner, 1995).

In the immediate vicinity of the flame we can estimate the characteristic times: $t_{\mathrm{coag}}$, $t_f$ and $t_T$, where, say

$$t_T = \left[ v_{p;z}(z) \cdot (d \ln T/dz) \right]^{-1} \approx 68 \text{ ms} \qquad (17)$$

Here $T(z)$ is obtained from thermocouple measurements (Xing et al., 1996, 1997, 1999), and $v_{p;z}(z) \approx 7.4$ cm/s is calculated from the estimated gas velocity at the flame $v_g(z_{FL}) \approx 12.6$ cm/s by subtracting off the thermophoretic velocity (Gomez and Rosner, 1993). The ratio of the first two times $t_{\mathrm{coag}}$ and $t_f$ is, of course, the *local* Damköhler number $\mathrm{Dam}_f$ for fusion. Keeping in mind the definition of $t_f$ *cf*. Eq. 5, a

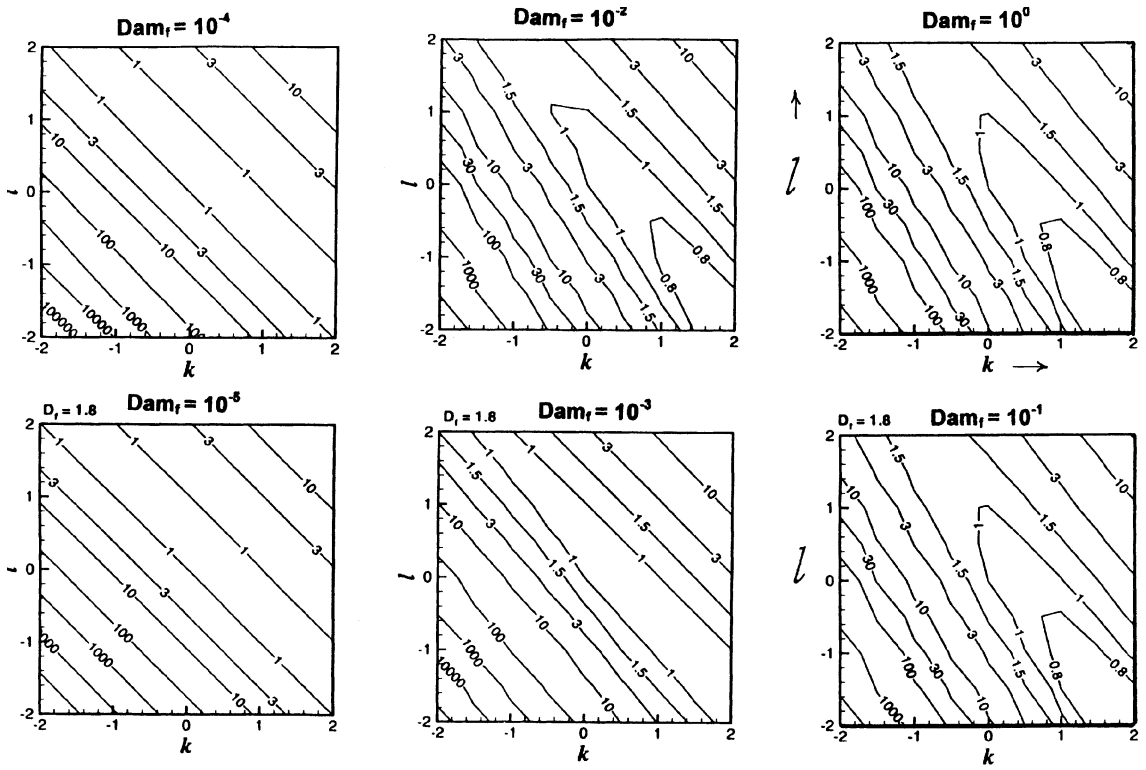


**Figure 11. Contours of constant dimensionless "mixed moments" on the *k*,*l* plane.**

Ensemble-averaged MC-predictions over a range of Damköhler numbers for pre-specified fractal dimension $D_f = 1.8$; Values of $(Dam)_f$ range from $10^{-5}$ (lower left) to 1 (upper right), in multiples of 10. (See also Rosner et al., 2000b).

"population"-mean fusion *time*, $\langle t_f \rangle$, can be calculated from the equation

$$\langle t_f \rangle = \left[ \bar{a} - a_{\min}(\bar{v}) \right] \Big/ \left[ -v_{p,z}(z) \cdot (d\,\bar{a}/dz) \right] \qquad (18)$$

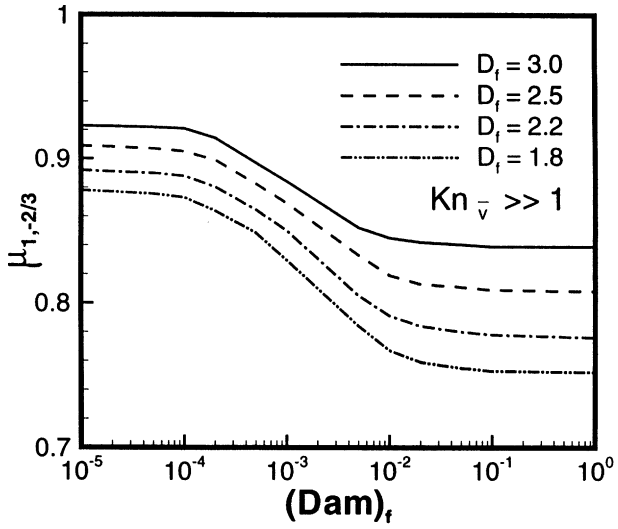


**Figure 12. Damköhler number dependence of the particular dimensionless moment $\mu_{1,-2/3}$ (relevant to *Sc* ≫ 1 Brownian deposition from the entire aerosol population).**

MC-predictions over a range of pre-specified fractal dimensions, $D_f$ between 1.8 and 3.

applied at, say, $z \approx 6.35$ mm [where $T \approx 2280$ K, $\bar{N}_{\text{eff}} = 36$ spherules [(*via* LLS), and $\bar{d}_{\text{l,eff}} = 27$ nm (*via* TPS/TEM)]. Assuming that

$$\bar{a} = \left[ \bar{a}/a_{\min}(\bar{v}) \right] \cdot a_{\min}(\bar{v}) = \left( \bar{N}_{\text{eff}} \right)^{1/3} \cdot a_{\min}(\bar{v}) \qquad (19)$$

and $\bar{v} = \bar{N}_{\text{eff}} \cdot \bar{v}_{\text{l,eff}}$, this can be conveniently written in terms of experimental observables

$$\langle t_f \rangle = \left\{ \bar{d}^2_{l,\text{eff}} \cdot \left[ \left( \bar{N}_{\text{eff}} \right)^{1/3} - 1 \right] \right\} \Big/ \left\{ -v_{p,z}[z] \cdot \left[ d\left( d^2_{l,\text{eff}} \bar{N}_{\text{eff}} \right)/dz \right] \right\} \qquad (20)$$

Inserting available local data on $\bar{N}_{\text{eff}}(z)$ and $\bar{d}_{\text{l,eff}}(z)$ (Xing et al., 1999) we find $\langle t_f \rangle \approx 1.5$ ms. Typical *aggregate* coagulation times in the immediate vicinity of the flame can also be estimated from the abovementioned observables (including the local alumina volume fraction of *ca*. 0.07 ppm), and the free-molecule regime Brownian coagulation frequency given earlier. In this way we find $t_{\text{coag}} \approx 150$ ms [this corrects the near-flame under-estimate of $t_{\text{coag}}$ in Figures 9 and 10 of, respectively, Xing (1996, 1997) (which were based on an *a priori* value for free spherules, rather than the measured *aggregates* at each $T(z)$)]. Thus, at this location in the flame structure (where the effects of high temperature fusion become noticeable *via* both TPS/TEM and LLS-data), $(\text{Dam})_f$ is of order 100, coagulation is slow compared to the rate of change of the environment, which is itself slow compared to

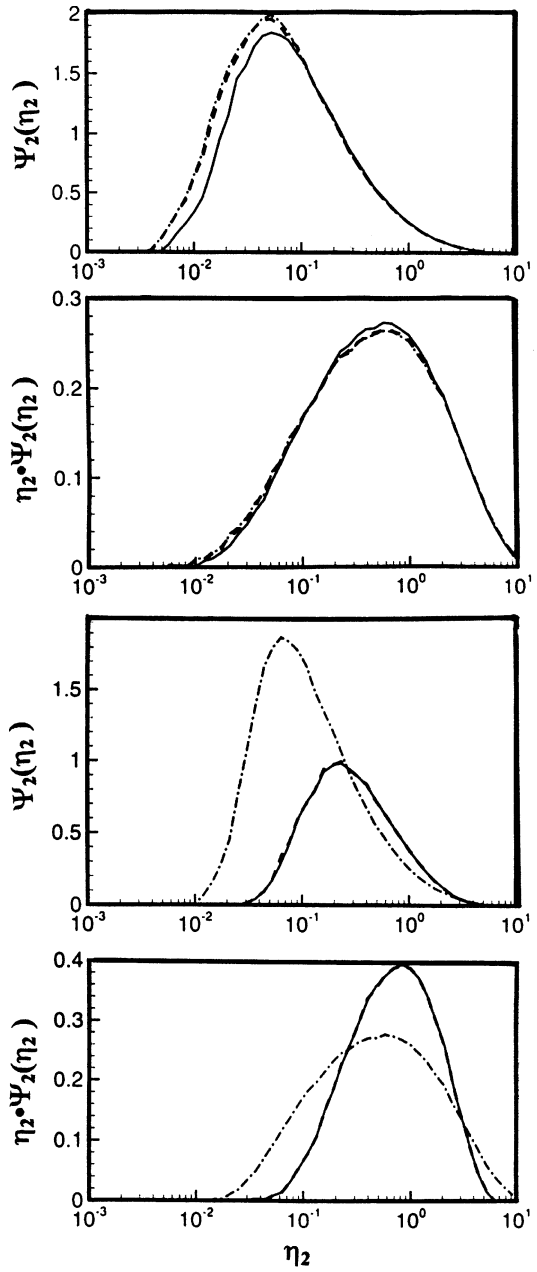


**Figure 13. Effect of sintering rate law (*cf.* const. $t_f$ (solid lines)).**

Viscous flow $t_f$ (dashed) and surface-diffusion $t_f$ (dot-dash) on the MC-predicted unconditional *pdf* with respect to scaled surface *area* for an aggregate population with $D_f = 1.8$. Extreme cases shown: (a) $\mathrm{Dam}_{f,t=0} = 10^{-5}$ (slow fusion; top two panels), and (b) $\mathrm{Dam}_{f,t=0} = 1$ (rapid fusion; bottom two panels).

the local sintering rate. Even allowing for the fact that the aggregate size distribution entering this "sintering" zone is already far from "mono-dispersed," the conditions for local "self-preservation" *with respect to volume* are marginal at best. Moreover, as shown in the next subsection, the time constant associated with the rate of change of the relevant Damköhler number is also much smaller than $t_{\mathrm{coag}}$ itself. These characteristic time inequalities evidently *preclude* local *quantitative* application of our present results (discussed in the last section) to the aerosol population prevailing in significant portions of the abovementioned flame structure. Yet, as discussed briefly below, certain important trends *are* captured, and the present techniques/information provide valuable background and experience before confronting a more accurate (but, in many respects, less general) formulation.

### *Temperature dependence of governing Damköhler number*

Brownian coagulation is not an "activated" rate process. In contrast, "sintering" by any of the mechanisms described earlier is associated with a significant molecular level energy barrier $E$ implying that the characteristic "fusion" time $t_f$, and the corresponding Damköhler number $(\mathrm{Dam})_f$ will be sharply temperature dependent. One corollary of this sensitivity is the rapid "onset" of appreciable fusion (sintering) in the vicinity of the flame. Phrased in another way, as the flame is approached, the "parameter" $(\mathrm{Dam})_f$ rapidly changes from $(\mathrm{Dam})_f \ll 1$ to $(\mathrm{Dam})_f \gg 1$ with a characteristic time that can be estimated as

$$t_{\mathrm{Dam}} \approx t_T \cdot [E/(RT)]^{-1} \tag{21}$$

where $t_T$ is the characteristic time for temperature-change (see above) and $E/(RT)$ is the associated *dimensionless activation energy,* probably of the order of 20 for, say, surface diffusion in the present case (Xing et al., 1996, 1997, 1999). This puts $t_{\mathrm{Dam}}$ in the range of only 3 ms, also much smaller than $t_{\mathrm{coag.}}$ locally. Accordingly, we should *not* expect our asymptotic ("self-preserving") solutions for $\Psi_{12}[\eta_1, \eta_2; (\mathrm{Dam})_f, D_f]$, in which $(\mathrm{Dam})_f$ is formally a constant "parameter," to apply *even locally* in our flame structure. It will also be seen that formally treating the ("population-averaged") morphological parameter $D_f$ as a constant "parameter" is also unrealistic, in that $D_f$ and $(\mathrm{Dam})_f$, will inevitably be "correlated" such that the function: $D_f[(\mathrm{Dam})_f]$ has the limiting behavior: $D_f(0) = 1.7$, whereas, clearly (in the rapid fusion limit) $D_f(\infty) = 3$.

### *TEM-derived "shape factor" and MC-results for the area-ratio parameter, $a/a_{min}(v)$, and associated $N_{eff}$*

Since $(\mu_{-2,+3})^{-1/3}$ is evidently not very different from unity, we expect $\bar{a}/a_{\mathrm{min}}(\bar{v})$ to "track" $(\bar{N}_{\mathrm{eff}})^{1/3}$. Thus, the rapid decay of the optically-inferred mean spherule number $\bar{N}$ from *ca.* 46 (at $z = 6$ mm) to 27 (at 6.7 mm) (Xing et al., 1999) corresponds to a drop in $\bar{a}/a_{\mathrm{min}}(\bar{v})$ from *ca.* 3.6 to 3.0, which can be located approximately along $D_f = 1.8$ contour in Figure 9, and, indeed, corresponds to a large increase in $(\mathrm{Dam})_f$. If Figure 9 were quantitatively applicable, one could read off the corresponding $(\mathrm{Dam})_f$-ratio and infer a meaningful activation energy for the fusion process. However, for the reasons indicated earlier, this cannot be justified *a posteriori*, and, if formally attempted, leads to systematically low E-values.

Similarly, the TEM image analysis aggregate local "shape factors" ("$C_{\mathrm{sf}}$") reported in Figure 8 of Xing et al., 1997, should track $[\bar{a}/a_{\mathrm{min}}(\bar{v})]^{3/2}$, so that these earlier data also indicate peak values of $\bar{a}/a_{\mathrm{min}}(\bar{v})$ near 3.4, with a rapid descent to values near 1.7 at the flame location (with some further spheroidization [it is interesting to note that the ultimate

(spheroidized) value of $\bar{a}/a_{\min}(\bar{v})$ *for the population* is not actually unity, but rather the moment $\mu_{2/3} \approx 0.923$ for the unconditional distribution with respect to *volume*] occurring on the downstream side of the hot flame). Again, this reduction in $\bar{a}/a_{\min}(\bar{v})$ corresponds to a large increase in $(\mathrm{Dam})_f$ (Figure 9), but quantitative use of this figure would *not* be self-consistent.

### $D_f$ evolution

Pre-specification of a population-averaged *fractal dimension* (morphology) parameter, independent of the Damköhler number governing sintering, is clearly "artificial." However, short of introducing a much more accurate way to deal with the collision frequency of nonspherical particles (Rosner, 1999), and as anticipated earlier it may be possible to extend the use of our present dimensionless results by imagining a (generally applicable?) "correlation" between the operative morphological parameter $D_f$ and the rate ratio parameter, $(\mathrm{Dam})_f$. While we know that $D_f(0) = 1.7$ and $D_f(\infty) = 3$, some experimental or theoretical basis for selecting the intermediate functional form of $D_f[(\mathrm{Dam})_f]$ would clearly be necessary. The fact that the population-averaged, optically inferred fractal dimension, as well as the mean number of spherules per aggregate, evolves in approximate accord with a prevailing Damköhler number is also evident in the recent angle-dependent laser light scattering measurements of Xing et al. (1999).

Despite the recently demonstrated utility of the mass fractal dimension $D_f$ as a robust morphology descriptor for (largely unsintered) aggregates in flames (Megaridis and Dobbins, 1990; Koylu et al., 1995, 1996; Liu et al., 1999) and other environments, our current view is that it may be possible to assign to each particle an "expected" or "effective" $D_f$ in accord with its ratio; $a/a_{\min}(v)$ and *its* $\mathrm{Dam}_f$. If so, $D_f$ would assume a subordinate role, being *dependent* on the "primary" state variables $v,a$, and not explicitly used to calculate either the rate of coagulation or the sintering rate. One additional output function of possible interest (to compare with available measurements) would then be $pdf(D_f)$, rather than its mean for the local population of nonspherical particles. Again, with the guidance provided by our laboratory flame observations using both thermophoretic sampling/TEM image-analysis, and *in situ* laser diagnostics (Xing et al., 1996, 1997, 1999), this subject will be taken up in our future theoretical work on the bi-variate problem of simultaneous coagulation and spheroidization outlined in the next subsection (Rosner et al., 2000; Rosner and Pyykonen, 2001).

### Transient multivariate formulation and laminar CDFs with axial thermophoresis

The discussions in this section up to this point lead us to conclude that the MC-predicted asymptotic results of the previous section only apply qualitatively to the alumina aerosols probed in our laboratory laminar counterflow diffusion flames. On the other hand, it is clear that the MC-simulation *method*, applied here in a constant environment at large $t/t_{\mathrm{coag}}$, can now be applied to the actual evolution problem, simultaneously allowing for rapid environmental changes, systematic improvement in the rate laws for coagulation and sintering, and the evolution of an effective, *distributed* fractal dimension. This more ambitious but probably instructive work, clearly beyond the scope of this article, is in progress.

## Conclusions

Choosing particle *volume* $v$ and "wetted" surface *area* $a$ as the basic independent particle "state" variables, and following up on our recent investigation of the *continuum*, long-time limit (Tandon and Rosner, 1999), we have quantitatively treated here Brownian coagulation in the *"free-molecule"* long-time limit, retaining the simplest analytic forms for the Brownian coagulation rate-, and sintering rate laws [in which $a - a_{\min}(v)$ is the "driving force" for surface area reduction]. When the aerosol environment is spatially uniform and time-invariant, we have shown that this combination of coagulation- and sintering-rate laws again leads to "self-preserving" rescaled *jpdf*s, and unconditional (marginal) *pdf*s, explicitly time-independent, but dependent on a Damköhler-like dimensionless parameter (constructed from the *ratio* of the characteristic *coagulation time* to the characteristic *sintering time*) for each pre-specified population fractal dimension (as discussed in earlier sections).

The free-molecule collision frequency law, corrected for the "fractal-like" character of flame-generated aggregates, is certainly more relevant to our aggregate evolution experiments in atmospheric pressure counterflow laminar flames (Xing et al., 1996, 1997, 1999). While actual flame environments are more complex than our present idealized simulations in several respects, our present dimensionless joint- and unconditional-*pdf*s, and associated "mixed" moments, do capture several important features of recent experimental results—especially the evolution of a particle "shape factor" (calculated from thermophoretically acquired sample TEM images of alumina aggregate cross-section and perimeter) as one approaches the flame (Xing et al., 1996, 1997, 1999) and the corresponding "collapse" of the average number of spherules per aggregate as one approaches the flame. Quantitative application of "local self-similarity" to particle populations evolving in our flame environments is evidently impossible, based on comparison between the prevailing time "constants" for coagulation and temperature change in our flames (Xing et al., 1997, 1999), when compared to the relaxation times associated with the approach to "self-preservation" (see previous section and Wright et al., 2001). Nevertheless, the abovementioned semi-quantitative agreement, coupled with the inherent versatility of such MC-simulation methods for multi-state variable population balances, encourages current extensions ultimately capable of providing: (a) realistic predictions of the performance of flame particle synthesis reactors (Pratsinis, 1998; Rosner, 1997, 2000b); (b) sintering rate parameter inferences from well-defined laboratory experiments of inorganic nano-aggregate *populations* restructuring in laminar flames (Rosner and Pyykonen, 2001).

More accurate rate laws for coagulation (Rosner, 2001) and sintering (Xing and Rosner, 1999), compatible with the $v,a$ state variable description employed here, are currently under development. They will be incorporated in our MC-based flame simulations, along with the weak size and morphology dependence of the particle thermophoretic diffusivity (Rosner et al., 1991, 2000a; Garcia-Ybarra and Rosner, 1989). However, even our present MC-simulation results (Tandon and

Rosner, 1999) can be used to develop and test the accuracy of bi-variate "moment"-based methods (McGraw, 1997; Wright et al., 2001; Rosner et al., 2000b) that would be particularly convenient for future parameter-estimation purposes. These methods, *inter alia*, are expected to lead to a rational versatile, yet tractable, formalism for future design calculations in the rapidly developing field of *sol reaction engineering* (SRE).

## Acknowledgments

It is a pleasure to acknowledge the financial support of NSF (Grant: CTS-987 1885). We also acknowledge helpful discussions/correspondence with P. Tandon, Y. Xing, J. L. Katz, U. O. Koylu, R. L. McGraw, R. B. Diemer Jr., A. V. Filippov, J. L. Castillo, J. Fernandez de la Mora, P. Garcia-Ybarra, A. G. Konstandopoulos, J. J. Pyykonen, C. M. Sorensen, D. Wright, and M. Zurita.

## Notation

$a$ = particle surface *area*
$a'''$ = aerosol population surface *area per unit volume* = $N_p \cdot \bar{a}$
$C_{sf}$ = population "shape factor" based on TEM projected areas and perimeters (see Xing et al., 1977)
$d_g$ = particle diameter corresponding to $v_g$
$d_l$ = spherule diameter ("primary" particles in aggregate)
$D_p$ = Brownian diffusion coefficient for particle of volume $v$
$D_s$ = surface diffusion coefficient (units: $m^2/s$)
$D_v$ = bulk diffusion coefficient (units: $m^2/s$)
$D_f$ = fractal exponent ("dimension") describing morphology of aggregate population
$E$ = activation energy barrier (aggregate restructuring)
$k_B$ = Boltzmann constant
$Kn_p$ = Knudsen number based on prevailing gas mean-free path and particle diameter
$l_g$ = gaseous *molecule mean free path*
$m_p$ = mass of particle of volume $v$
$n$ = size distribution function $dN_p/dv \cdot da$
$N_{eff}$ = number of "spherules" in an aggregate; $v/v_{1,eff}$
$N_p$ = total particle number density
$R_l$ = radius of spherule
$\mathfrak{R}$ = deposition rate ratio (Eq. 16)
$Sc$ = particle Schmidt number, $(\mu/\rho)_{gas}/D_p$
$t_f$ = characteristic fusion (coalescence) time
$T$ = absolute temperature (Kelvins)
$u$ = particle volume (dummy variable); see, also, $v'$
$v$ = volume of condensed material in spherical particle or aggregate
$v_g$ = geometric-mean particle volume in log-normal PSD $n(v, \ldots)$
$\bar{v}$ = mean particle volume, $\phi_p/N_p$, of local aerosol
$v_{1,eff}$ = effective spherule volume, computed from $d_{1,eff} = 6v/a$
$v_m$ = average molecular volume in condensed state
$z$ = axial position in flame structure
$\beta(u,v)$ = coagulation rate constant in "mass-action" law (used to calc. coag. time)
$\delta$ = effective thickness of surface layer; approx: $3(6v_m/\pi)^{1/3}$
$\eta_1$ = dimensionless particle *volume*, $v/\bar{v}$(t)
$\eta_2$ = dimensionless particle *area*, $a/\bar{a}$(t)
$\phi_p$ = particle volume fraction; $\bar{v} \cdot N_p$
$\kappa$ = number of coagulation events in MC simulation; *cf*. Figure 1
$\rho_p$ = intrinsic density of a particle $(m_p/v_p)$
$\mu_{kl}$ = dimensionless "mixed" moment of dimensionless PSD: $\Psi_{12}$ (Eq. 15)
$\mu_{gas}$ = dynamic Newtonian viscosity of the carrier gas
$\mu$ = dynamic Newtonian viscosity of condensed material
$\Psi_1$ = dimensionless unconditional *pdf* with respect to rescaled *volume* v
$\Psi_2$ = dimensionless unconditional *pdf* with respect to rescaled dimensionless *area*, a
$\Psi_{12}$ = dimensionless joint *pdf* with respect to dimensionless volume and area
$\sigma_g$ = geometric standard deviation of the unconditional *pdf* with respect to volume or area
$\sigma$ = surface energy ("tension") of condensed material
$\nu$ = momentum diffusivity ("kinematic viscosity") of the carrier gas, $(\mu/\rho)_{gas}$

### *Subscripts*

BU = breakup
$c$ = continuum limit ($Kn_p \ll 1$) (Tandon and Rosner, 1999)
coag = coagulation
coalesc = coalescence
eff = effective value
$f$ = fusion (coalescence)
FL = at gaseous flame "sheet"
fm = free-molecule limit ($Kn_p \gg 1$)
$g$ = pertaining to log-normal PSD (geometric)
gas = pertaining to the carrier gas
gyr = gyration
$k,l$ = pertaining to moment exponents $k,l$, where $k,l$ need *not* be an integer, nor positive
$m$ = pertaining to a single molecule
max = maximum value
min = minimum value
$N$ = pertaining to nucleation
$p$ = particle(s)
ref = reference value; $a_{ref} \equiv a_{min}(v) = 4\pi[3v/(4\pi)]^{2/3}$
$T$ = thermophoretic; or based on $T(z)$
1 = pertaining to the "primary" spherules ($d_{1,eff} = 6v/a$)
1 = pertaining to particle *volume* (*cf*. area) as in $\eta_1$, $\Psi_1$
2 = pertaining to particle *area* (*cf*. volume) as in $\eta_2$, $\Psi_2$

### *Miscellaneous*

$(\,)''$ = per unit area
$(\cdot)$ = time rate of change
$(-)$ = mean value of $(\,)$ ($\bar{v}$, $\bar{a}$, $\bar{N}$, ...)
$(\,)'$ = dummy variable, as in $\beta(v,v',a,a')$ pertaining to collision partner
min $(a, b)$ = lesser of $a$, $b$
| = conditioned on (given: ); Figures 6 and 7
c = continuum limit ($Kn_p \ll 1$)
coag = pertaining to (Brownian) coagulation
CDF = counterflow diffusion flame (Xing et al., 1996, 1997, 1999)
CPU = central processor unit
*Dam* = Damköhler number (characteristic *time* ratio); $t_{coag}/t_{fusion}$
*fm* = free-molecule limit ($Kn_p \gg 1$)
IPDE = integro-partial differential equation
*jpdf* = joint probability density function (here bi-variate)
LLS = laser light scattering
MC = Monte Carlo
mfp = gaseous *molecule mean free path*
ODE = ordinary differential equation
*pdf* = probability density function (normalized)
PSD = particle size (volume) distribution
RHS = righthand side
SRE = sol reaction engineering
TEM = transmission electron microscopy
TPS = thermophoretic sampling
(),[] = arguments of indicated function

## Literature Cited

Bird, G. A, *Molecular Gas Dynamics and the Direct Simulation of Gas Flows*, Clarendon, Oxford (1994).
Cohen, E. R., and E. U. Vaughn, "Approximate Solution of the Equations of Aerosol Agglomeration," *J. Colloid. Interface Sci*., **35**, 612 (1971).
Diemer, R. B., Jr., "Moment Methods for Coagulation, Breakage and Coalescence Problems," PhD Diss., Chemical Engineering Dept., Univ. of Delaware (1999).
Dobbins, R. A., and C. M. Megaridis, "Morphology of Flame-Gener-

ated Soot as Determined by Thermophoretic Sampling," *Langmuir*, **3**, 254 (1987).
Dobbins, R. A., and G. Mulholland, "Interpretation of Optical Measurements of Flame-Generated Particles," *Comb. Sci. Tech.*, **40**, 175 (1984).
Filippov, A. V., M. Zurita, and D. E. Rosner, "Fractal-Like Aggregates: Relation Between Morphology and Physical Properties," *J. Colloid Interface Sci.*, **229**, 261 (Sept. 2000).
Flagan, R. C., and M. M. Lunden, "Particle Structure Control in Nano-Particle Synthesis From the Vapor Phase," *Mat. Sci. and Eng.*, **A204**, 113 (1995).
Flagan, R. C., and J. H. Seinfeld, *Fundamentals of Air Pollution Engineering*, Prentice Hall, Englewood Cliffs, NJ (1988).
Frenklach, M., and S. Harris, "Aerosol Dynamics by the Method of Moments," *J. Colloid. Int. Sci.*, **118**(1), 252 (1987).
Friedlander, S. K., *Smoke, Dust and Haze*, Oxford University Press, New York (2000).
Garcia-Ybarra, P., and D. E. Rosner, "Thermophoretic Properties of Non-spherical Particles and Large Molecules," *AIChE J.*, **35**, 139 (1989).
Garcia-Ybarra, P., and J. L. Castillo, "Mass Transfer Dominated by Thermal Diffusion in Laminar Boundary Layers," *J. Fluid Mech.*, **336**, 379 (1997).
Gooch, J. R. P., and M. J. Hounslow, "MC Simulation of Size-Enlargement Mechanisms in Crystallization," *AIChE J.*, **42**, 1864 (1996).
Gomez, A., and D. E. Rosner, "Thermophoretic Effects on Particles in Counterflow Laminar Diffusion Flames," *Comb. Sci. Tech.*, **89**, 335 (1993).
Helble, J. J., "Combustion Aerosol Sintering of Nano-scale Ceramic Powders," *J. Aerosol Sci.*, **29**, (5,6) 721 (1998).
Helble, J. J., and A. F. Sarofim, "Factors Determining the Primary Particle Size of Flame-Generated Inorganic Aerosols," *J. Colloid Interface Sci.*, **128**, 348 (1989).
Hulburt, H. M., and S. Katz, "Some Problems in Particle Technology: A Statistical Mechanics Formulation," *Chem. Eng. Sci.*, **19**, 555 (1964).
Hung, C.-H., and J. L. Katz, "Formation of Mixed Oxide Powders in Flames: I. $TiO_2$-$SiO_2$," *J. Mater. Res.*, **7**(7), 1861 (1992).
Koch, W., and S. K. Friedlander, "The Effect of Particle Coalescence on the Surface Area of a Coagulating Aerosol," *J. Coll. Interface Sci.*, **140**, 419 (1990).
Koylu, U. O., Y. Xing, and D. E. Rosner, "Fractal Morphology Analysis of Combustion-Generated Aggregates Using Angular Light Scattering and Electron Microscope Images," *Langmuir*, **11**, 4848 (1995).
Koylu, U. O., "Quantitative Analysis of *in situ* Optical Diagnostics for Inferring Particle/Aggregate Parameters in Flames: Implications for Soot Surface Growth and Total Emissivity," *Comb. Flame*, **109**, 488 (1997).
Kruis, F. E., A. Maisels, and H. Fissan, "Direct Simulation Monte Carlo Method for Particle Coagulation and Aggregation," *AIChE J.*, **46**(9), 1735 (2000).
Landgrebe, J. D., and S. E. Pratsinis, "A Discrete-Sectional Model for Particulate Production by Gas-Phase Chemical Reaction and Aerosol Coagulation in the Free-Molecular Regime," *J. Colloid Int. Sci.*, **39**, 63 (1990).
Liu, B. B., S. Srinivasachar, and J. J. Helble, "The Effect of Chemical Composition on Fractal-like Structure of Combustion-Generated Inorganic Aerosols," *Aerosol Sci. Tech.*, **33**, 459 (2000).
Lu, S. Y., "Collision Integrals of Discrete-Sectional Model in Simulating Powder Production," *AIChE J.*, **40,** 1761 (1994).
McGraw, R. L., "Description of Aerosol Dynamics by the Quadrature Method of Moments (QMOM)," *Aerosol Sci. Tech.*, **27**, 255 (1997).
Meakin, P., "Computer Simulation of Growth and Aggregation Processes," *On Growth and Form*, H. E. Stanley and N. Ostrowsky, eds., NATO ASI Series E100, Martinus Nijhoff Publishers, Boston, MA, p. 111 (1987).
Megaridis, C. M., and R. A. Dobbins, "Morphological Description of Flame-Generated Materials," *Comb. Sci. Tech.*, **71**, 95 (1990).
Mulholland, G. W., R. J. Samson, R. D. Mountain, and M. H. Ernst, "Cluster Size Distribution for Free-Molecular Agglomeration," *J. Energy Fuels*, **2**, 481 (1988).
Mullins, M. W., "Mass Transport at Interfaces in Single Component Systems," *Metal. Material Trans.*, **A26**, 1917 (1995).
Neimark, A. V., U. O. Koylu, and D. E. Rosner, "Extended Characterization of Combustion-Generated Aggregates: Self-Affinity and Lacunarities," *J. Colloid Int. Sci.*, **180**, 590 (1996).
Oh, C., and C. M. Sorensen, "Light Scattering Study of Fractal Cluster Aggregation Near the Free Molecular Regime," *J. Aerosol Sci.*, **28**, 937 (1997).
Papadopulos, D. H., and D. E. Rosner, "Enclosure Gas Flows Driven by Non-isothermal Walls," *Physics of Fluids*, **7**, 2535 (1995).
Pope, S., "PDF Methods for Turbulent Reacting Flows," *Progress in Energy and Comb. Sci.*, **11**, 119 (1985).
Pratsinis, S. E., "Flame Aerosol Synthesis of Ceramic Powders, " *Progress in Energy and Comb. Sci.*, **24**, 197 (1998).
Ramkrishna, D., *Population Balances — Applications to Particulate Systems in Engineering*, Academic Press, Orlando, FL (2000).
Randolph, A. D., and M. A. Larson, *Theory of Particulate Processes — Analysis and Techniques of Continuous Crystallization*, Academic Press, New York (1988, 1971).
Rosner, D. E., "Combustion Synthesis and Materials Processing," *Chem. Eng. Educ.*, **34**, 228 (1997).
Rosner, D. E., "Knudsen Transition-Effects on Total Mass Deposition Rates From 'Coagulation-Aged' Aerosol Populations," AIChE Particle Technology Forum, *Proc. Symp. on Advanced Technologies for Particle Production.*, Miami Beach, FL, **1**, 357 (Nov. 15–20, 1998).
Rosner, D. E., *Transport Processes in Chemically Reacting Flow Systems*, 4th printing, Dover Publications, Mineola, NY (2000a).
Rosner, D. E., "Method for Predicting Brownian Coagulation Rates of Non-Spherical Particles in the Continuum or Free-Molecule Regimes," in press (2001).
Rosner, D. E., "Aerosol Reaction Engineering: Measuring and Modeling the Performance of Combustion-Synthesized Nano-particle Reactors," Plenary Lecture for AAAR2000, St. Louis, MO (Nov. 2000).
Rosner, D. E., and M. Tassopoulos, "Deposition Rates from 'Polydispersed' Particle Populations of Arbitrary Spread," *AIChE J.*, **35,** 1497 (1989).
Rosner, D. E., and M. Tassopoulos, "Direct Solutions to the Canonical 'Inverse' Problem of Aerosol Sampling Theory: Coagulation and Size-Dependent Wall Loss Corrections for Log-normally Distributed Aerosols in Upstream Sampling Tubes," *J. Aerosol Sci.*, **22**, 843 (1991).
Rosner, D. E., P. Garcia-Ybarra, and D. W. Mackowski, "Size and Structure-Insensitivity of the Thermophoretic Transport of Aggregated 'Soot' Particles in Gases," *Comb. Sci. Tech.*, **80**, 87 (1991).
Rosner, D. E., and Y. F. Khalil, "Morphology Effects on Polydispersed Aerosol Deposition Rates," *Trans. Amer. Nuc. Soc.*, **77**, TANSAO 77-1-560, 425 (1997).
Rosner, D. E., and Y. F. Khalil, "Particle Morphology- and Knudsen Transition Effects on Thermophoretically Dominated Total Mass Deposition Rates From 'Coagulation-Aged' Aerosol Populations," *J. Aerosol Sci.*, **31**(3), 273 (2000).
Rosner, D. E., and H. M. Park, "Thermophoretically Augmented Mass-, Momentum- and Energy- Transfer Rates in High Particle-Loaded Laminar Forced Convection Systems," *Chem. Eng. Sci.*, **43**, 2689 (1988).
Rosner, D. E., D. W. Mackowski, M. Tassopoulos, J. L. Castillo, and P. Garcia-Ybarra, "Effects of Heat Transfer on the Dynamics and Transport of Small Particles in Gases," *I&EC-Res.*, **31**, 760 (1992).
Rosner, D. E., P. Tandon, A. G. Konstandopoulos, and M. Tassopoulos, "Prediction/Correlation of Particle Deposition Rates From Dilute Polydispersed Flowing Suspensions and the Nature/Properties of Resulting Deposits," *Proc. 1st Int. Particle Technology Forum*, Paper 68h, Denver, CO, AIChE, IChE, Vol. II, p. 374 (Aug., 1994).
Rosner, D. E., and P. Tandon, "Prediction and Correlation of Accessible Area of Large Multi-Particle Aggregates," *AIChE J.*, **40,** 1167 (1994).
Rosner, D. E., D. W. Mackowski, and P. Garcia-Ybarra, "Size- and Structure-Insensitivity of the Thermophoretic Transport of Aggregated 'Soot' Particles in Gases," *Comb. Sci. Tech.*, **80**, 87 (1991).
Rosner, D. E., J. J. Pyykonen, R. L. McGraw, and D. L. Wright, "Bivariate Moment Method Simulation of a Population of Coagu-

lating and Sintering Alumina Nano-particles in a Laminar Diffusion Flame," AAAR2000, St. Louis, MO (Nov., 2000a).
Rosner, D. E., P. Tandon, R. L. McGraw, and D. L. Wright, "Relevant 'Mixed Moments' for the Calculation of Deposition, Vapor Scavenging and Optical Properties of Populations of Non-Spherical Suspended Particles," *AIChE Proc. Particle Technology Forum*, Session Tld08 (Nov., 2000b).
Rosner, D. E., and J. J. Pyykonen, "Bi-variate Moment Method Simulation and Measurement of Populations of Coagulating and Sintering Alumina Nano-particles in Laminar Counterflow Diffusion Flames," *AIChE J.*, in press (2001).
Smith, M., and T. Matsoukas, "Constant Number Monte-Carlo Simulation of Population Balances," *Chem. Eng. Sci.*, **53**, 1777 (1998).
Sorensen, C. M., and G. M. Wang, "Size Distribution Effect on the Power Law Regime of the Structure Factor for Fractal Aggregates," *Phys. Rev. E*, **60**, 7143 (1999).
Sweet, I. R., S. S. Gustafson, and D. Ramkrishna, "Population-Balance Modelling of Bubbling Fluidized Bed Reactors—I. Well-Stirred Dense Phase," *Chem. Eng. Sci.*, **42**, 341 (1987).
Tandon, P., and D. E. Rosner, "Co-Deposition on Hot CVD-Surfaces: Particle Dynamics and Deposit Roughness Interactions," *AIChE J.*, **42,** 1673 (1996).
Tandon, P., and D. E. Rosner, "Monte-Carlo Simulation of Particle Aggregation and Simultaneous Restructuring," *J. Colloid Interface Sci.*, **213**, 273 (1999).
Tandon, P., and D. E. Rosner, "Translational Brownian Diffusion Coefficient of Large (Multi-particle) Suspended Aggregates," *Ind. Eng. Chem.-Res.*, **34**, 3265 (1995).
Tandon, P., and D. E. Rosner, "Sintering Kinetics and Transport Property Evolution of Large Multi-Particle Aggregates," *Chem. Eng. Commun.*, **151**, 147 (1996).
Ulrich, G. D., and N. S. Subramanian, "Particle Growth in Flames: III. Coalescence as a Rate-Controlling Process," *Comb. Sci. Tech.*, **17**, 119 (1977).
Vemury, S., K. A. Kusters, and S. E. Pratsinis, "Time-Lag for Attainment of the Self-Preserving Size Distribution by Coagulation," *J. Colloid Int. Sci.*, **165**, 53 (1994).
Vemury, S., and S. E. Pratsinis, "Self-Preserving Size Distributions of Agglomerates," *J. Aerosol Sci.*, **175**, 175 (1995).
Williams, M. M. R., and S. K. Loyalka, *Aerosol Science and Theory*, Pergamon Press, New York (1991).
Wright, D. L., R. L. McGraw, and D. E. Rosner, "Bivariate Extension of the Quadrature Method of Moments For Modeling Simultaneous Coagulation and Particle Sintering," *J. Colloid Int. Sci.*, in press (2001).
Wright, H., and D. Ramkrishna, "Solution of Inverse Problems in Population Balances: I. Aggregation Kinetics," *Computers in ChE*, **16**, 1019 (1992).
Wu, M. K., and S. K. Friedlander, "Enhanced Power-Law Agglomerate Growth in the Free-Molecule Regime," *J. Aerosol Sci.*, **24**, 273 (1993).
Wu, J. J., and R. C. Flagan, "A Discrete-Sectional Solution to the Aerosol Dynamic Equation," *J. Colloid Int. Sci.*, **123**, 339 (1988).
Xing, Y., U. O. Koylu, and D. E. Rosner, "Synthesis and Restructuring of Inorganic Nano-particles in Counterflow Diffusion Flames," *Comb. & Flame*, **107**, 85 (1996).
Xing, Y., U. O. Koylu, P. Tandon, and D. E. Rosner, "Morphological Evolution of Oxide Nano-particles in Laminar Counterflow Diffusion Flames—Measurements/Modelling," *AIChE J.*, **43,** 2641 (1997).
Xing, Y., and D. E. Rosner, "Prediction of Spherule Size in Gas Phase Nano-particle Synthesis," Invited Paper for *J. Nano Particle Res.* (Special Issue on Gas Phase Synthesis of Nano-Particle), **1**, 277 (1999).
Xing, Y., U. O. Koylu, and D. E. Rosner, "*In Situ* Light Scattering Measurements of Morphologically Evolving Flame-Synthesized Oxide Nano-Aggregates," *J. Applied Optics*, **38**, 2686 (1999).
Xiong, Y., and S. E. Pratsinis, "Formation of Agglomerate Particles by Coagulation and Sintering: 1-A, Two-dimensional Solution of the Population Balance Equation," *J. Aerosol Sci.*, **24**, 283 (1993).
Yang, G., and P. Biswas, "Study of the Sintering of Nano-sized Titania Agglomerates in Flames Using *in situ* Light Scattering Measurements," *Aerosol Sci. Tech.*, **27**, 507 (1997).
Yu, S., and I. M. Kennedy, "A Two-Dimensional Discrete-Sectional Model for Aerosol Nucleation and Growth in a Flame," *Aerosol Sci. Tech.*, **28**, 185 (1998).
Yu, S., and I. M. Kennedy, "An Approximate Method to Approximate the Collision Rates of Discrete-Sectional Model," *Aerosol Sci. Tech.*, **27**, 266 (1998).
Yu, S., P. Tandon, and D. E. Rosner, "Time to Achieve 'Self-Preservation' for Populations of Non-spherical Particles which are Simultaneously Coagulating and Sintering," in press (2001).
Zachariah, M. R., and H. G. Semerjian, "Simulation of Ceramic Particle Formation: Comparison With *in situ* Experiments," *AIChE J.*, **35,** 2003 (1989); ["Silica Particle Synthesis in a Counterflow Diffusion Flame Reactor," *Comb. & Flame*, **78**, 287 (1989).]

*Manuscript received May 17, 1999, and revision received Sept. 12, 2000.*